

CHAPTER 4

Characterization of Unplasticized MC-NH₄NO₃ Polymer Electrolyte System

4.1 Introduction

The attention given towards research in polymer-salted complexes is due to their possible application as solid electrolytes in electrochemical devices. Pioneering studies began in the seventies when poly (ethylene oxide) (PEO) doped with alkali metal salt exhibited ionic conductivity [Hashmi *et al.*, 1990]. Considering the drawbacks of PEO which can easily recrystallize at room temperature, the search for newer, better and environmental friendlier systems have been pursued in the past many years.

The aim of the present chapter is to develop a new type of proton-conducting polymer electrolyte (PE) with high conductivity at room temperature using methyl cellulose. The minimum conductivity sought for is 10^{-5} S cm⁻¹. Methyl cellulose (MC), a biodegradable polymer was used as host and NH₄NO₃ (AN) salt as the source for protons. The prepared PEs have been characterized using x-ray diffraction (XRD), Fourier transform infrared (FTIR) spectroscopy, thermogravimetric analysis (TGA) and electrochemical impedance spectroscopy (EIS).

4.2 X-ray diffraction (XRD) analysis

Figure 4.1 depicts the XRD patterns of the MC-NH₄NO₃ system at room temperature.

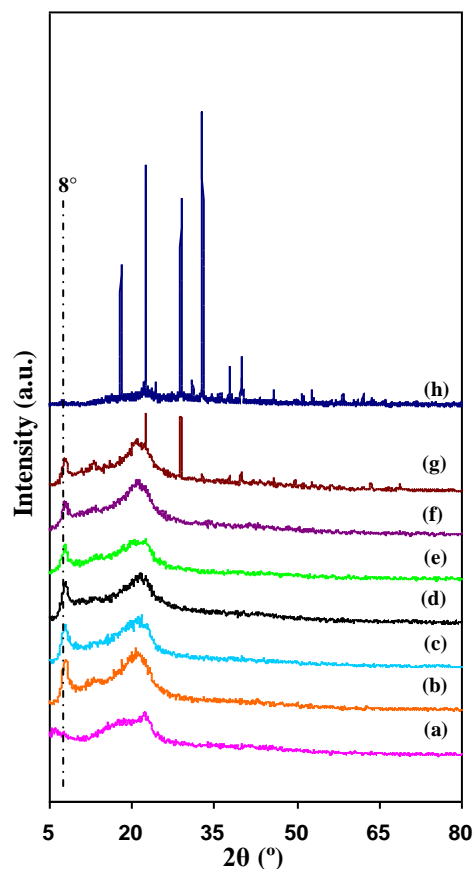


Figure 4.1: XRD diffractogram for (a) pure MC, (b) 95MC5AN, (c) 90MC10AN, (d) 85MC15AN, (e) 80MC20AN, (f) 75MC25AN, (g) 70MC30AN, (h) pure AN (NH₄NO₃)

The broad peak in the $9^\circ \leq 2\theta \leq 25^\circ$ range in Figure 4.1 indicates some intermolecular structure order of this polymer and can be associated with the amorphous nature of pure MC. On addition of 5 wt.% to 30 wt.% of AN, a small peak, can be observed at $2\theta = 8^\circ$. The diffractogram shown in Figure 4.1 (g) exhibit peaks attributed to AN at $2\theta \sim 22^\circ$ and 28° indicating that the salt has recrystallized out of the host [Shuhaimi *et al.*, 2010]. Hence it can be implied that on addition of AN greater than 25 wt.% a two-phase system is

produced. It may be predicted that the sample with 25 wt.% should exhibit the highest room temperature conductivity. The increase and/or decrease in amorphousness can be justified by calculating the crystalline fraction in the samples using the x-ray diffractograms. According to Hodge *et al.* (1996), the crystalline fractions in the samples were predictable from the ratio of the integrated intensity of peaks associated with crystalline reflections to the integrated area of the spectrum by the equation below:

$$X_C = \frac{I_C}{I_T} \times 100\% \quad (4.1)$$

where X_C is crystalline fraction, I_T and I_C are the total and crystalline integrated intensities respectively.

The degree of crystallinity of the samples with salt concentration was evaluated using the above equation and listed in Table 4.1.

Table 4.1: Data of the degree of crystallinity of the samples

Salt concentration (wt.%)	I_C	I_T	X_C (%)
5	0.0278	0.7275	3.8213
10	0.0227	0.6227	3.6454
15	0.0227	0.6592	3.4436
20	0.0185	0.5659	3.2691
25	0.0172	0.7125	2.4140
30	0.0133	0.4568	2.9116

The decrease of the crystalline fractions of the samples with salt concentration from 5 to 25 wt.% AN reveals that the amorphousness of the polymer-salt complex system increases up to 25 wt.% AN. The increase in crystallinity for 75MC30AN is indicative that

this sample has a lower room temperature conductivity compared to 75MC25AN. Amorphous nature gives new coordination sites into which the ions may transit on migration. It is implied that the activation energy of 70MC30AN is higher than 75MC25AN.

To confirm the XRD results, we characterized our samples using Fourier transform infrared (FTIR) analysis to see whether MC and NH₄NO₃ have interacted or otherwise.

4.3 Fourier Transform Infrared (FTIR) analysis

FTIR was used to identify the nature of bonding in the samples by monitoring the vibrational energy levels of the molecules, which are essentially the fingerprint of different molecules [Rajendran *et al.*, 2007]. Following Osman and Arof (2003), information from FTIR can be used to predict chemical processes, identify species and determine the increase in the number of certain entities from the increase in the area of the band. In this work, FTIR was used to determine the possible interactions between MC and NH₄NO₃ in unplasticized polymer electrolytes system. Figure 4.2 and Table 4.2 present the FTIR spectrum and the vibrational modes in the spectrum of pure MC film in region of 700 to 3900 cm⁻¹.

Lin *et al.* (2007) reported that the region from 900 to 1500 cm⁻¹ is the finger-print region for MC. Velazquez *et al.* (2003) assigned the region from 1270 to 1500 cm⁻¹ to vibration modes of MC groups.

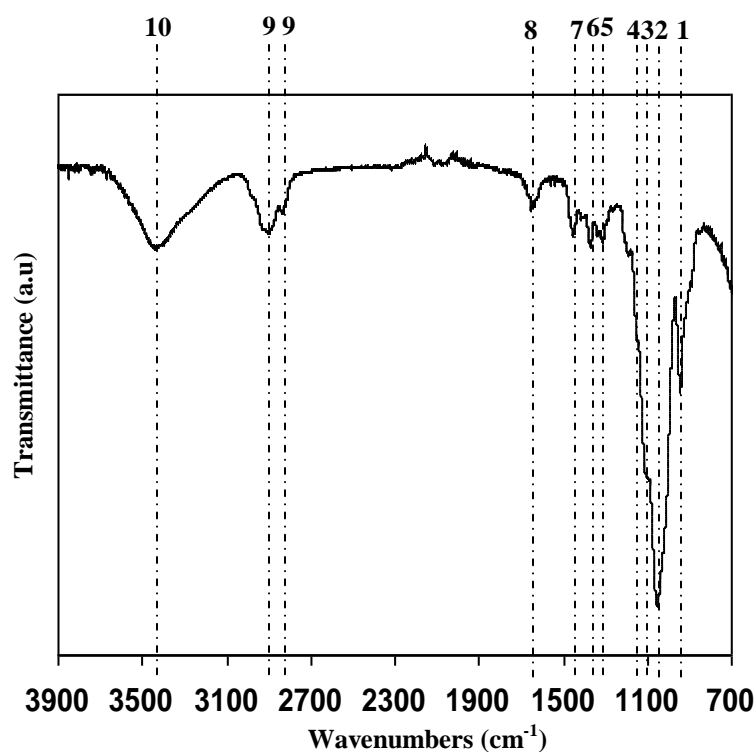


Figure 4.2: FTIR spectra for pure MC

Table 4.2: Vibrational modes with corresponding wavenumbers for pure MC

No.	Wavenumber (cm ⁻¹)	Assignment
1	944	-
2	1053	Skeletal vibration involving the C-O stretch
3	1112	Anti-symmetric stretching of the C-O-C
4	1152	C-O stretching from asymmetric oxygen bridge
5	1314	-
6	1374	C-H bending
7	1458	-
8	1580-1700	Bending mode of water molecule
9	2838, 2902	C-H stretching
10	3440	O-H stretching

- The infrared spectral characterization for MC which is similar with reported by Filho *et al.*, 2007

From Figure 4.2, the FTIR spectrum of MC film shows absorption at 1053 cm⁻¹ (skeletal vibration involving the C-O stretch), 1112 cm⁻¹ (asymmetric stretching of the C-

O-C groups of MC structure), 1152 (C-O stretching from asymmetric oxygen bridge), 1374 cm⁻¹ (C-H bending mode of MC), 2838 and 2902 cm⁻¹ (C-H stretching vibration), and 3440 cm⁻¹ (O-H stretching). The band positions are almost similar to those reported by some authors [Lin *et al.*, 2007; Yin *et al.*, 2006; Liu *et al.*, 2004; Chattopadhyay and Mandal, 1996; Rimdusit *et al.*, 2008; Filho *et al.*, 2007; Pinotti *et al.*, 2007; Babu *et al.*, 2007; Rokhade *et al.*, 2007]. There are also peaks in wavenumber range from 1580 to 1700 cm⁻¹, which according to Velazquez *et al.* (2003), correspond to bending mode of water molecules contained in the MC film. This result is also comparable with that reported by Lin *et al.* (2007), who reported the bending mode of water molecules in MC film at 1649 cm⁻¹. The bands at 944, 1314 and 1458 cm⁻¹ are also the infrared spectral characterization in MC [Filho *et al.*, 2007].

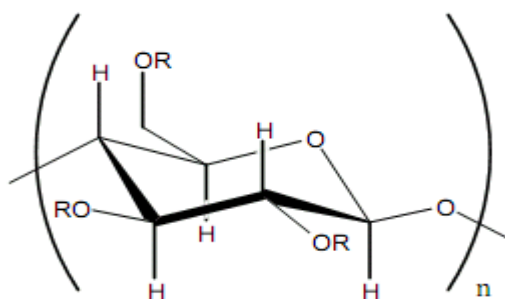


Figure 4.3: Methyl cellulose structure (Desbrières *et al.*, 2000). R is H or CH₃.

Knowledge on the vibration modes of pure MC is important in order to determine the location of O-H and C-O as can be seen in Figure 4.3. Complexation with charge carriers from salt can occur at the oxygen atom of these functional groups. Hence, bands at 3440 cm⁻¹ (O-H), 1053 cm⁻¹ (C-O) and 1314 cm⁻¹ will be checked for change in position, intensity and shape.

Ammonium nitrate (NH₄NO₃) or in short; AN, is a proton donor which has been used in the preparation of polymer electrolytes [Hema *et al.*, 2009; Majid *et al.*, 2005; Kadir *et al.*, 2010]. Figure 4.4 and Table 4.3 present the FTIR spectrum and the assignment of vibrational modes in the spectrum of pure AN in the region 700 to 3900 cm⁻¹.

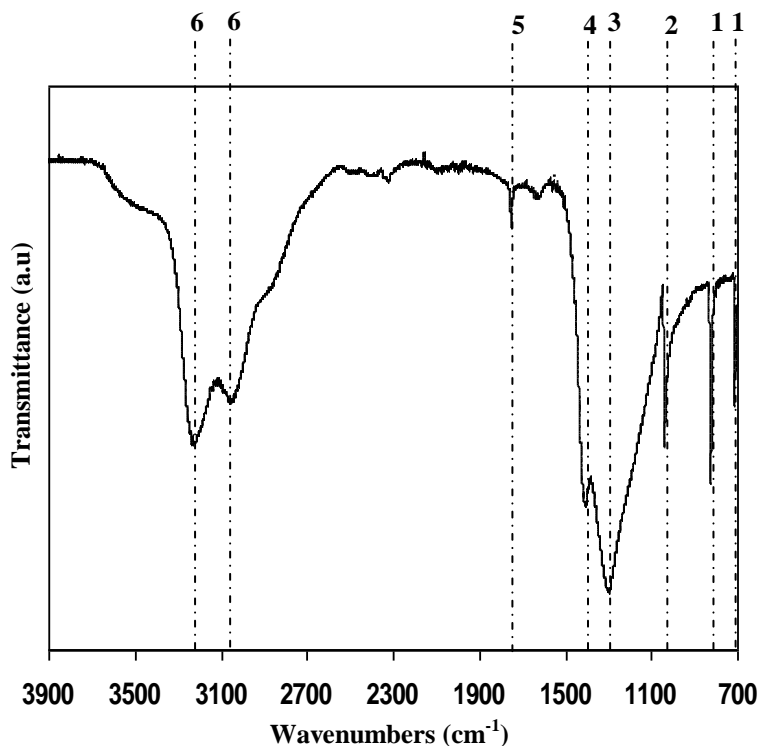


Figure 4.4: FTIR spectra for pure AN

It can be seen that the vibrational bands at 715 and 827 cm⁻¹ correspond to $\delta(\text{NO}_2)$ of NO_3^- , while 1300 and 1042 cm⁻¹ are attributed to $\nu_s(\text{NO}_2)$ and $\nu(\text{NO})$ of 'free' nitrate ions. The peaks at 1407 and 1419 cm⁻¹ are assigned to a mixture of $\nu_a(\text{NO}_2)$ of NO_3^- in AN and H-N-H bending of NH_4^+ vibration [Majid, 2007; Ramya *et al.*, 2008a]. The peak observed at 1754 cm⁻¹ is due to $\nu(\text{NH}_4^+)$ of pure AN [Majid and Arof, 2005]. The strong and intense peaks detected at 3058 and 3236 cm⁻¹ are ascribed to N-H stretching [Hashmi *et al.*, 1990; Ramya *et al.*, 2008a; Singh *et al.*, 2005].

Table 4.3: Vibrational modes with corresponding wavenumbers for pure AN

No.	Wavenumber (cm ⁻¹)	Assignment
1	715, 827	$\delta(\text{NO})_2$ of NO_3^-
2	1042	$\nu(\text{NO})$ of free nitrate ions
3	1300	$\nu_s(\text{NO}_2)$ of free nitrate ions
4	1407, 1419	A mixture of $\nu_a(\text{NO}_2)$ of NO_3^- and H-N-H bending of NH_4^+
5	1754	$\nu(\text{NH}_4^+)$
6	3058, 3236	Symmetric and asymmetric stretching of NH_4^+

Analysis of the FTIR spectra of the MC-NH₄NO₃ complexes is presented in Figure 4.5 in the region 700 to 900 cm⁻¹.

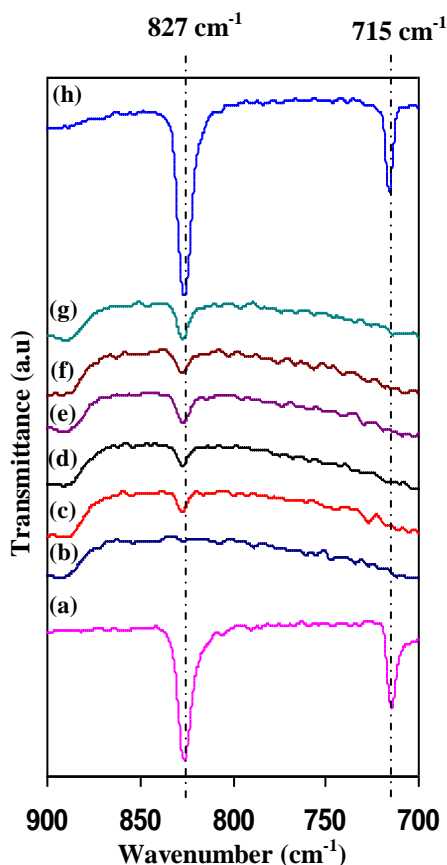


Figure 4.5: FTIR spectra for (a) pure AN, (b) pure MC, (c) 95MC5AN, (d) 90MC10AN, (e) 85MC15AN, (f) 80MC20AN, (g) 75MC25AN, (h) 70MC30AN in the spectral region of 700 to 900 cm⁻¹.

It can be seen that for pure MC, there are no peaks in this region. For pure AN there are two characteristic peaks at 715 and 827 cm⁻¹ which have been assigned to $\delta(\text{NO}_2)$ for a

'free' nitrate ion. The peak at 715 cm⁻¹ is found to be absent on addition of 5 to 25 wt.% AN (Figure 4.5 (c) to (g)). The disappearance of this peak proves that complexation has occurred in the MC-NH₄NO₃ system. For the sample with 30 wt.% salt (Figure 4.5 (h)), the same peak was observed at the same wavenumber. The presence of this peak at higher concentration of the salt could be attributed to the presence of ion pairs or ion aggregates.

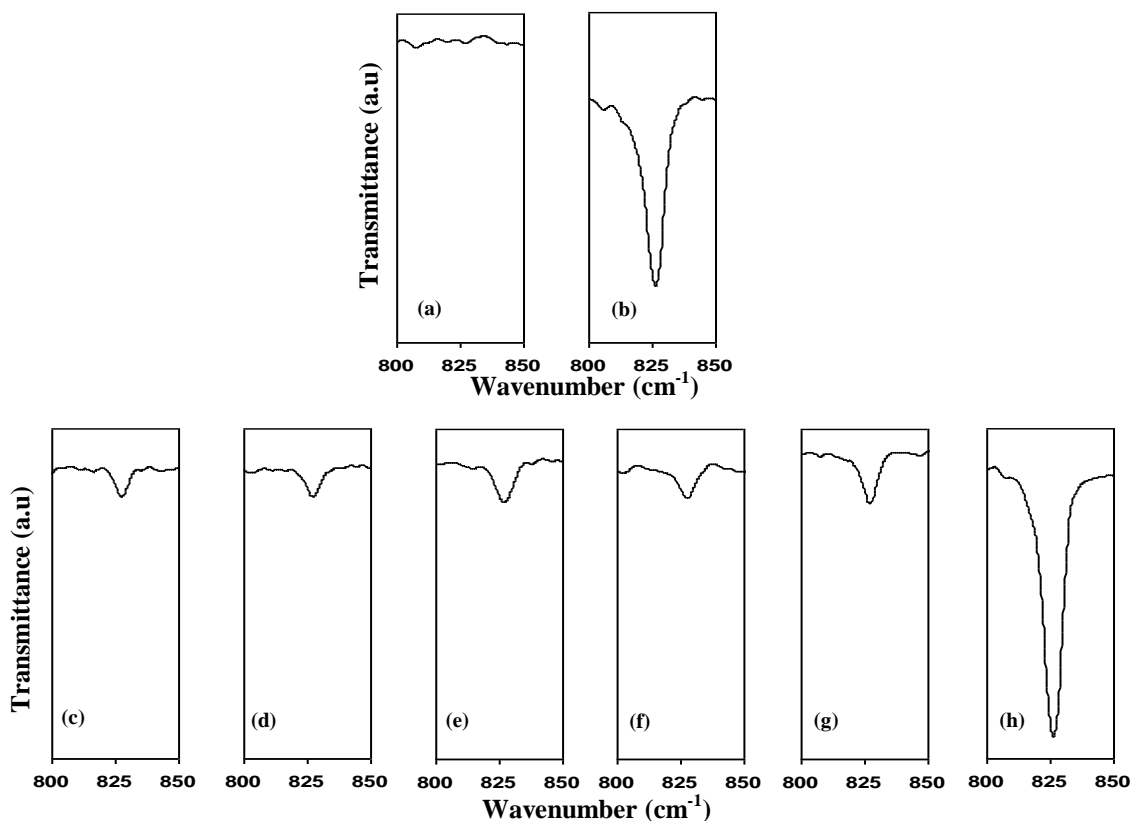


Figure 4.6: FTIR spectra for (a) pure MC, (b) pure AN, (c) 95MC5AN, (d) 90MC10AN, (e) 85MC15AN, (f) 80MC20AN, (g) 75MC25AN, (h) 70MC30AN in the spectral region of 800 to 850 cm⁻¹.

On the other hand, a peak at 827 cm⁻¹ gets more intense with addition of salt from 5 to 30 wt.% as depicted in Figure 4.5 and the spectrum is shown separately in Figure 4.6. This again provides evidence of complexation in MC-NH₄NO₃ complexes. The increase in intensity of this peak shows the increase in the number of charge carriers with the addition

of salt [Subban and Arof, 2004]. This result is also consistent with XRD results shown earlier.

In order to observe interactions between polymer and salt, the locations or sites of polar groups in the polymer host must be determined first. The region between 1000 and 1250 cm⁻¹ (Figure 4.7) is where vibrational modes of C-O stretching bands of MC can be located.

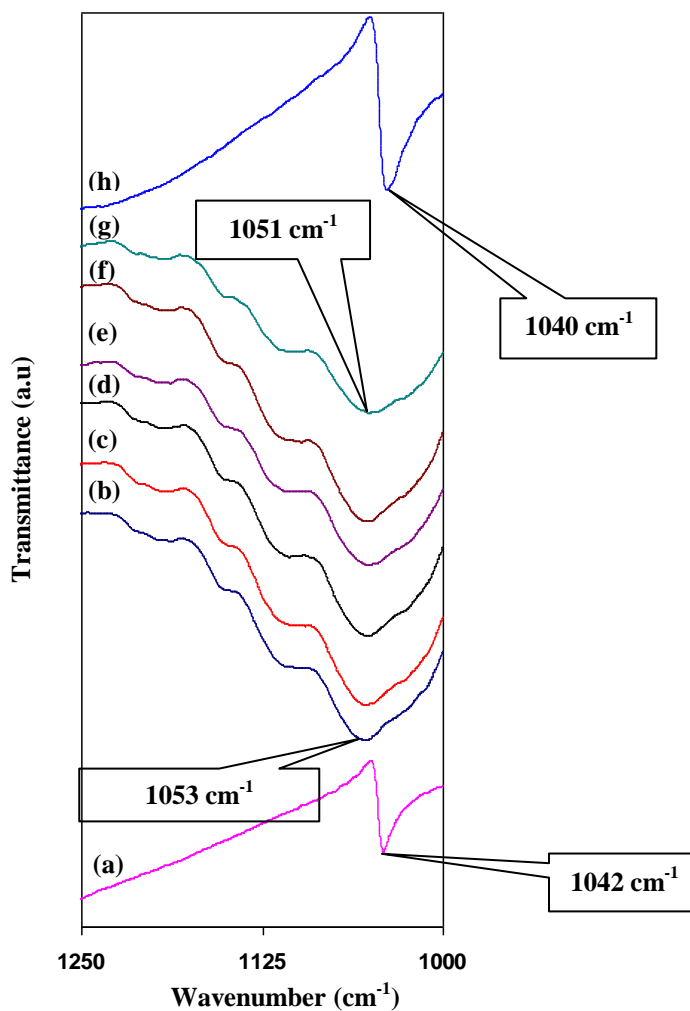


Figure 4.7: FTIR spectra for (a) pure AN, (b) pure MC, (c) 95MC5AN, (d) 90MC10AN, (e) 85MC15AN, (f) 80MC20AN, (g) 75MC25AN, (h) 70MC30AN in the spectral region of 1000 to 1250 cm⁻¹.

In pure MC, a peak at 1053 cm⁻¹ is assigned to the C-O stretching modes. With an increase in the salt concentration the peak was shifted to 1051 cm⁻¹ for sample containing 25 wt.% AN. This shift indicates that the complexation between MC and AN has taken place due to coordination of NH₄⁺ with the polar group in the MC structure of the MC-NH₄NO₃ complexes. A similar effect was reported by Reddy *et al.* (2000) for the poly(ethylene oxide) complexed with tetra-methyl-ammonium bromide based system. With high concentration of salt (Figure 4.7 (h)), the C-O stretching bands in MC structure and $\nu_a(\text{NO}_2)$ of NO₃⁻ in AN were observed to overlap and form a new peak at 1040 cm⁻¹. This overlapping peak is proof that the complexation between MC and AN has occurred.

According to Srivastava and Chandra (2000), the proton conduction can occur either by vehicular mechanism which involved NH₄⁺ motion or by the lone proton migration (Grotthus) mechanism. Two of the four hydrogen of NH₄⁺ ions are bound identically; third hydrogen is bound more rigidly and the fourth hydrogen more weakly. The weakly bound H⁺ in NH₄⁺ is due to the low difference in electronegativity and hence it can be easily dissociated under the influence of a dc electric field. The scheme of the ammonium nitrate is shown in Figure 4.8.

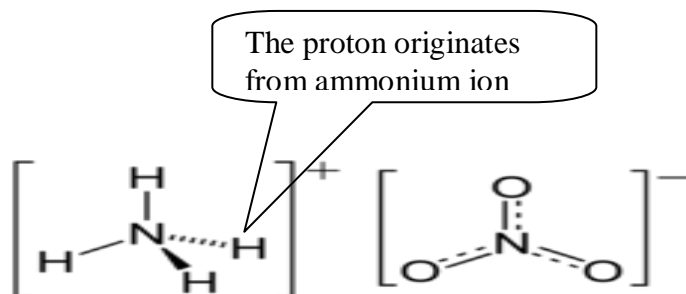
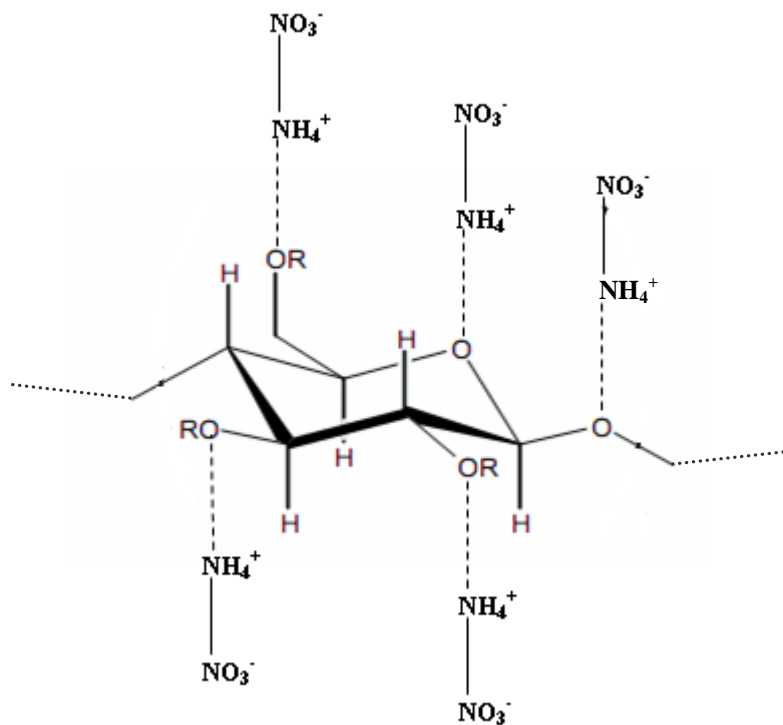


Figure 4.8: Ammonium nitrate (AN) structure

In this work, it can be deduced that the mechanism of proton conduction occurs via Grotthus mechanism when these H⁺ ions hop via each coordinating site (example; oxygen) of the host polymer (MC) and thus conduction take place as shown in Figure 4.9.



where R is H or CH₃

Figure 4.9: Schematic representation of the coordination of proton in MC-NH₄NO₃ polymer complex

The interactions between MC and NH₄NO₃ occurs when the nitrogen atom of the NH₄⁺ group is expected to interact with the oxygen present in the O-H and C-O groups in MC. At this stage complexation or interaction has occurred at 1053 cm⁻¹ (at the location of the C-O stretching modes in MC).

Figures 4.10 and 4.11 show the FTIR spectra of the same system in the region from 1200 to 1500 cm⁻¹. In this region, pure MC has three characteristic peaks at 1314, 1374 and

1458 cm⁻¹ which represents the infrared spectral of MC. Pure AN exhibits vibrational peaks at 1300 cm⁻¹ due to $\nu_s(\text{NO}_2)$ of NO_3^- in AN. The peaks at 1407 and 1419 are assigned to a mixture of $\nu_a(\text{NO}_2)$ of NO_3^- in AN and H-N-H bending of NH_4^+ vibration.

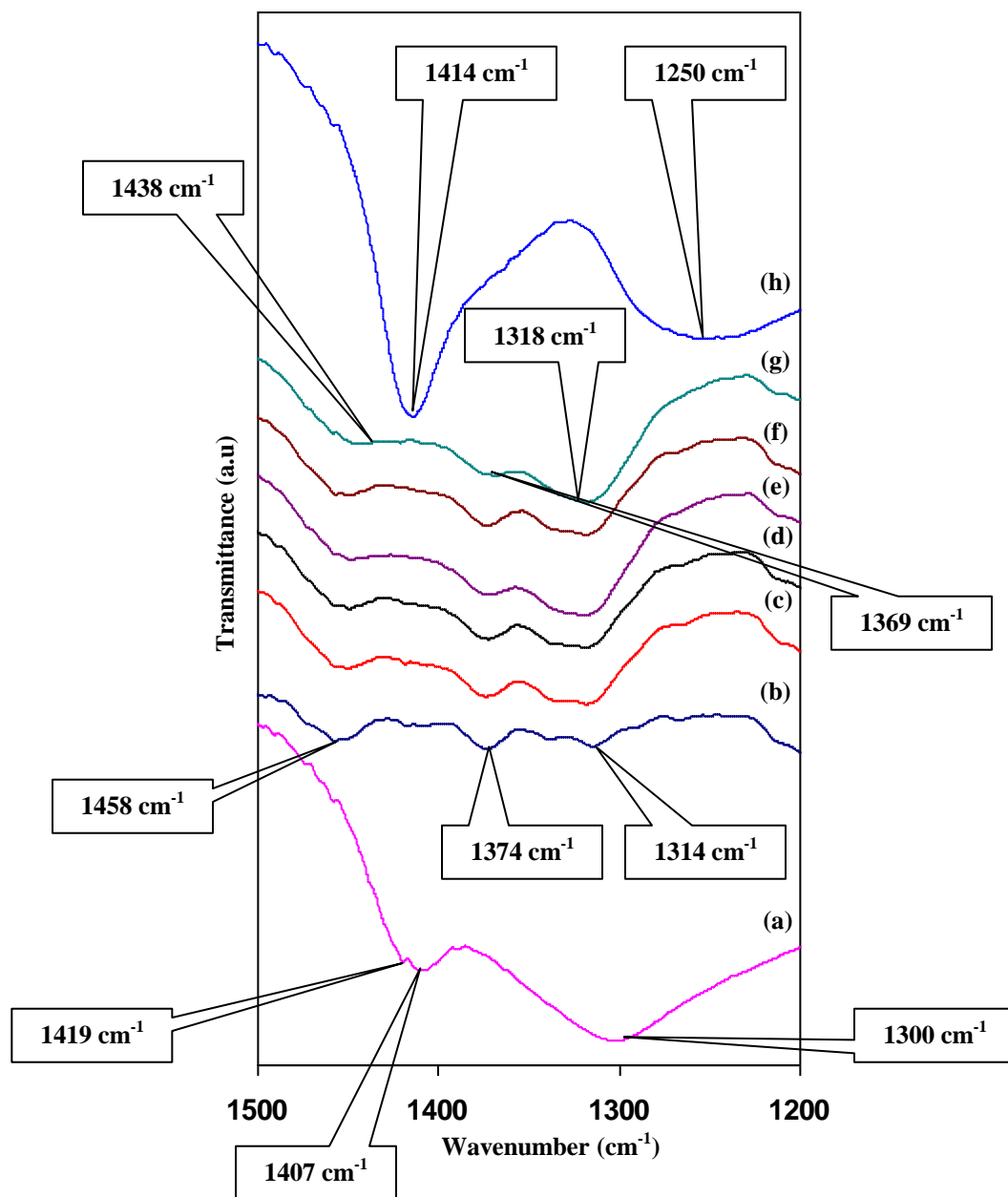


Figure 4.10: FTIR spectra for (a) pure AN, (b) pure MC, (c) 95MC5AN, (d) 90MC10AN, (e) 85MC15AN, (f) 80MC20AN, (g) 75MC25AN, (h) 70MC30AN in the spectral region of 1200 to 1500 cm⁻¹.

The intensity of the three peaks present in MC in the region from 1200 to 1500 cm⁻¹ seems to increase with addition of salt up to 25 wt.%. With increase in salt concentration, the three peaks shifted to 1318, 1369 and 1438 cm⁻¹. This is another proof that the complexation has occurred in MC-NH₄NO₃ system again. Beyond 25 wt.%, the characteristic peaks of MC are observed to overlap with vibrational peaks of NH₄NO₃. Thus, only a sharp peak is observed at 1414 cm⁻¹ with a shoulder at 1250 cm⁻¹.

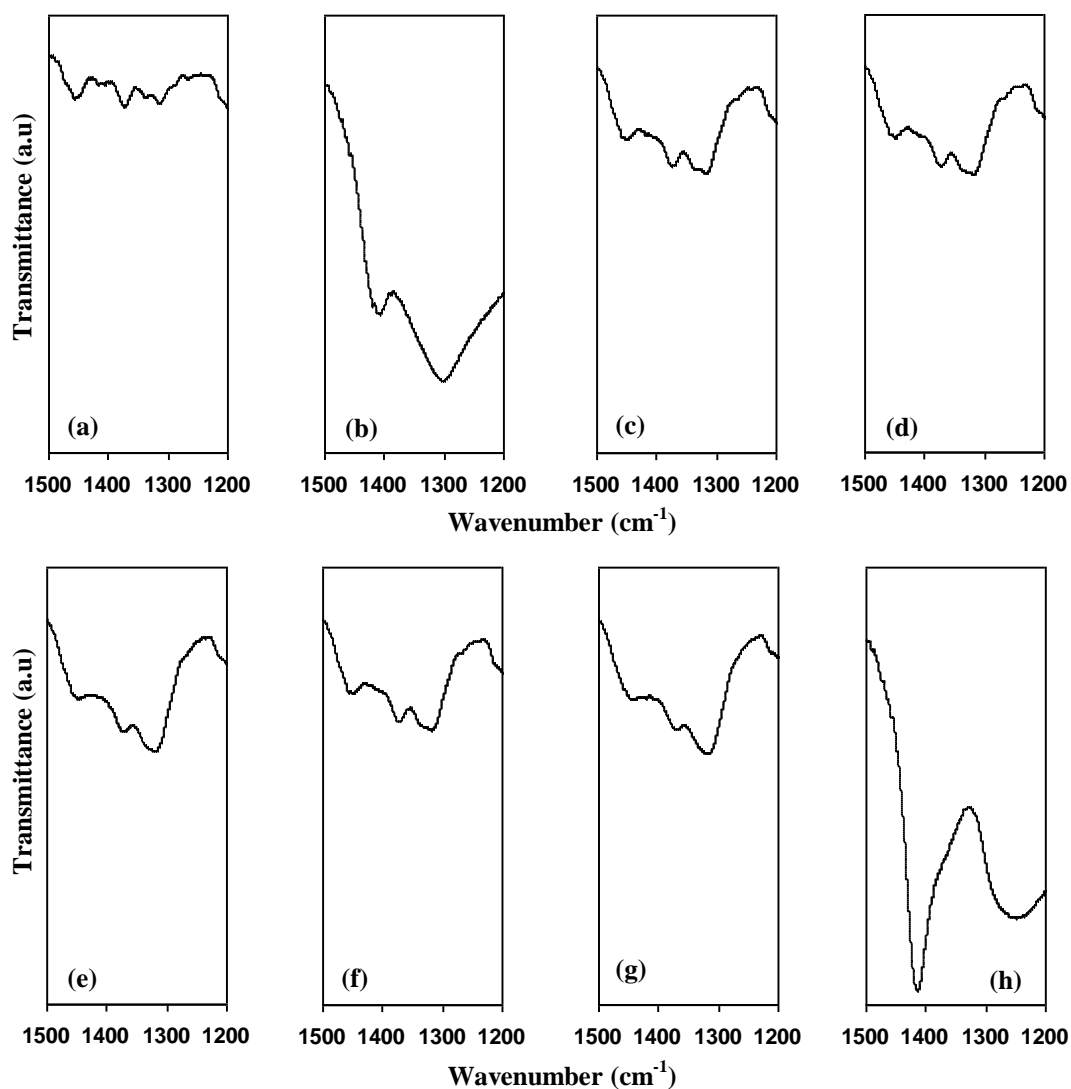


Figure 4.11: FTIR spectra for (a) pure MC, (b) pure AN, (c) 95MC5AN, (d) 90MC10AN, (e) 85MC15AN, (f) 80MC20AN, (g) 75MC25AN, (h) 70MC30AN in the spectral region of 1200 to 1500 cm⁻¹.

Figure 4.12 shows the FTIR spectrum of pure MC, pure AN and MC doped with AN for salt concentrations between 5 and 30 wt.% in the wavenumber range 1730 to 1770 cm⁻¹.

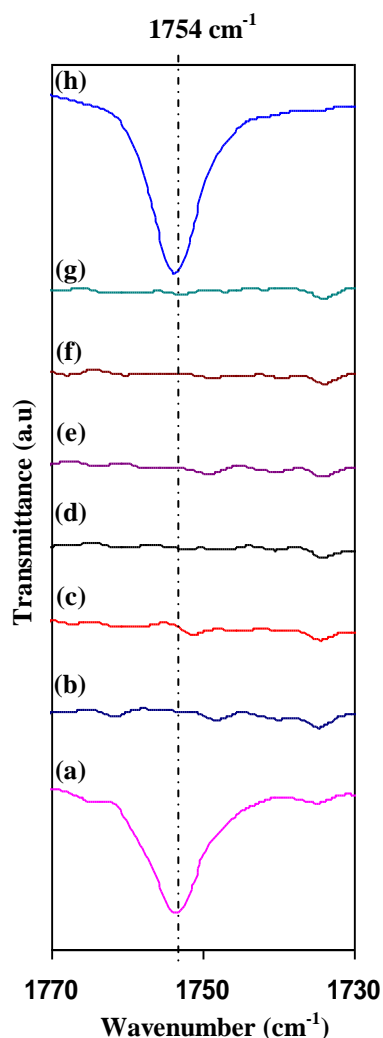


Figure 4.12: FTIR spectra for (a) pure AN, (b) pure MC, (c) 95MC5AN, (d)90MC10AN,(e)85MC15AN, (f) 80MC20AN, (g) 75MC25AN, (h) 70MC30AN in the spectral region of 1730 to 1770 cm⁻¹.

In this region, the peak at 1754 cm⁻¹ is due to $\nu(\text{NH}_4^+)$ in pure AN and no peaks are observed for pure MC in this region. With addition of AN from 5 to 25 wt.%, no new peaks appear. However, for the sample containing 30 wt.% AN, (Figure 4.12 (h)), a similar peak as in the spectrum of pure AN was observed. This result supports the XRD result for 70MC30AN, which showed crystallization peaks due to AN. Since recrystallization takes

place in this sample, this means that, concentration of charge carriers is reduced and this sample is expected to have conductivity lower than the 75MC25AN sample. Since the salt has recrystallized out of the sample, it absorbs infrared light and the spectrum shows the 1754 cm⁻¹ peak.

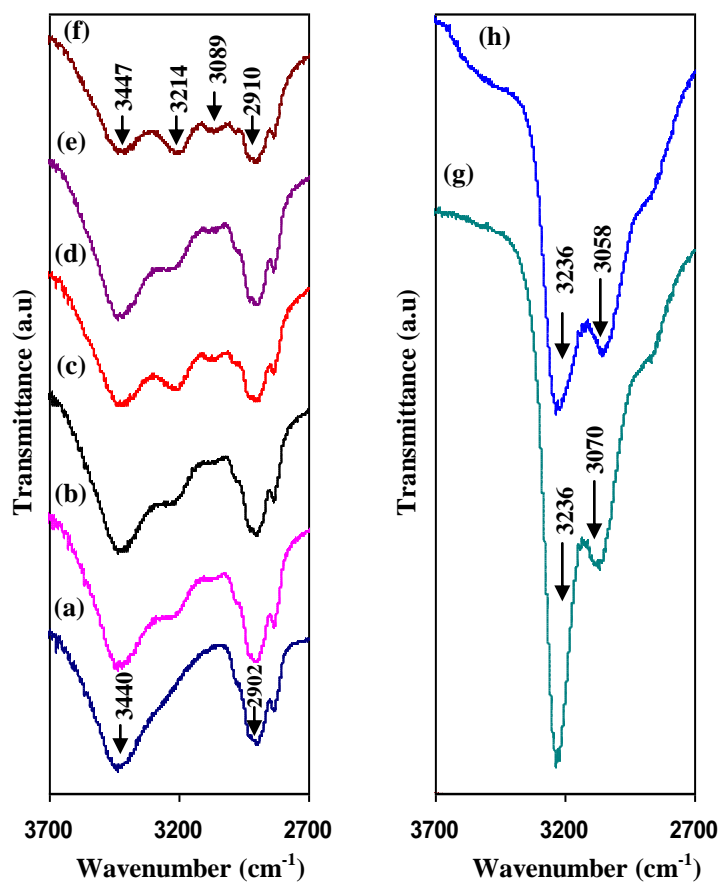


Figure 4.13: FTIR spectra for (a) pure MC, (b) 95MC5AN, (c) 90MC10AN, (d) 85MC15AN, (e) 80MC20AN, (f) 75MC25AN, (g) 70MC30AN, (h) pure AN in the spectral region of 2700 to 3700 cm⁻¹.

Figure 4.13 represents the spectrum of MC-NH₄NO₃ complexes in the region 2700 to 3700 cm⁻¹. It can be observed that OH stretching of pure MC is at 3440 cm⁻¹. On addition of 25 wt.% NH₄NO₃, the band shifted to lower wavenumber, 3437 cm⁻¹. In the spectrum of pure AN, the NH stretching has been detected at 3058 and 3236 cm⁻¹. The NH stretching was observed when the amount of salt increases from 5 to 30 wt.%. On addition

of 25 wt.% NH₄NO₃, the NH stretching shifted to 3214 and 3080 cm⁻¹. The spectrum of 70MC30AN showed almost same feature with pure AN spectrum but NH stretching at 3058 cm⁻¹ shifted to 3070 cm⁻¹.

4.4 Thermogravimetric analysis (TGA)

TGA analysis was employed in order to ascertain the thermal stability (decomposition pattern and thermal degradation), phase transition and crystallization of the polymer electrolytes [Rajendran *et al.*, 2004]. The effect of NH₄NO₃ in MC will also be revealed using TGA. Figure 4.14 shows the TGA curves of the MC-NH₄NO₃ complexes which exhibit percentage weight loss versus temperature. Table 4.4 gives the details of thermal behavior according to the thermograms in Figure 4.14. Figure 4.14 (a) shows the thermal degradation process that occurred in two stages for pure MC film. During the first stage sample starts to lose mass at temperatures below 125 °C. The weight loss in this temperature region for pure MC and doped samples is attributed to free water loss [Andrade *et al.*, 2009] or due to the evaporation of unbound water [Zohuriaan and Shokrolahi, 2004]. This indicates that all samples contain some free water in the matrix. The second stage weight loss occurs at DTGA_{max} = 321 °C with large decrease of mass corresponding to the structural degradation of MC. These results are good agreement with that reported by Filho *et al.* (2007) although in their work, they prepared methyl cellulose from sugar cane but the thermal properties of their sample is similar to commercial methyl cellulose. Similar results also were reported for methyl cellulose stability by Zohuriaan and Shokrolahi (2004), Tunç and Duman (2011), Park and Ruckestein (2001) and Rimdusit *et al.* (2008).

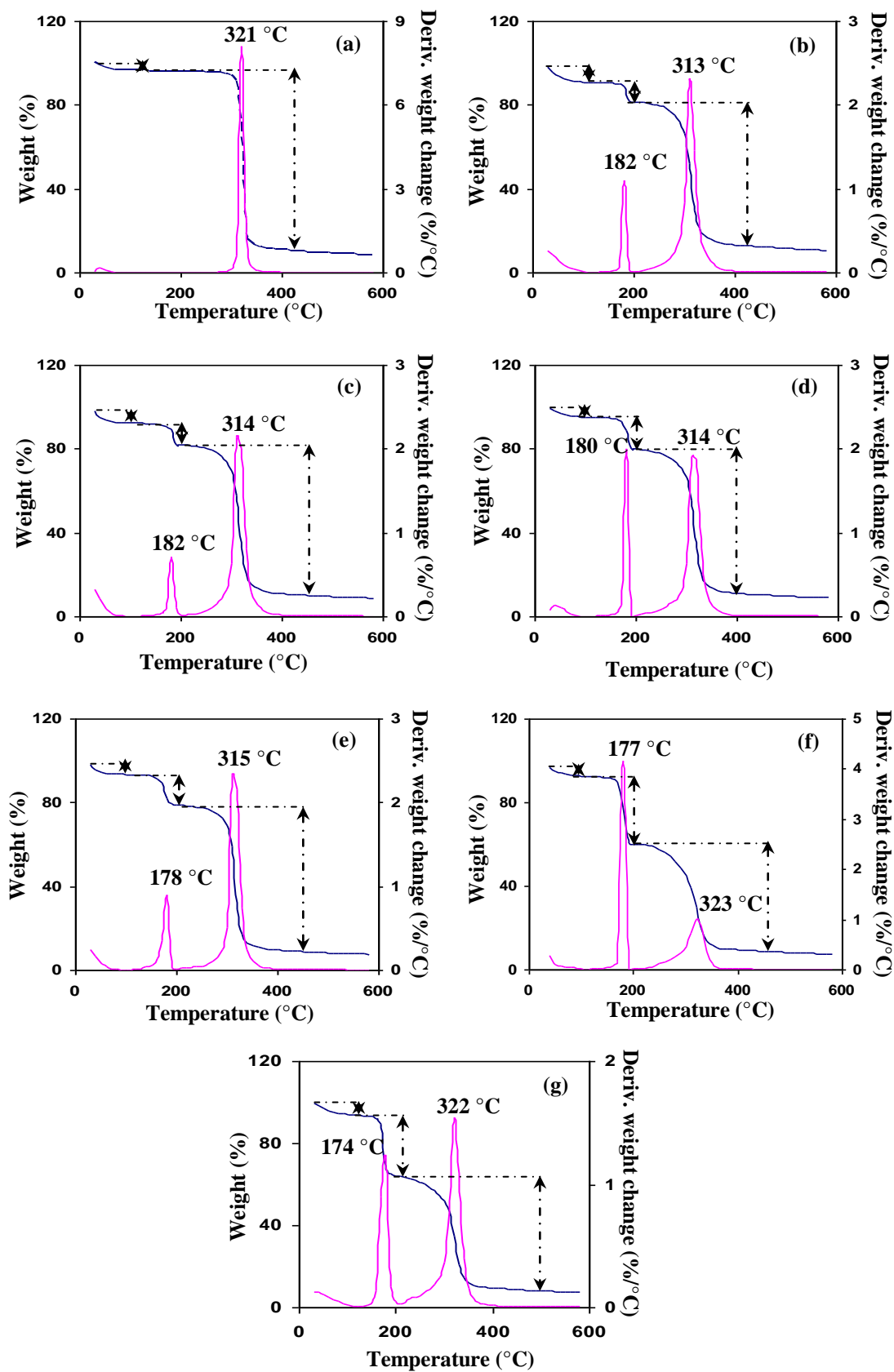


Figure 4.14: TGA curve for (a) pure MC, (b) 95MC5AN, (c) 90MC10AN, (d) 85MC15AN, (e) 80MC20AN, (f) 75MC25AN, (g) 70MC30AN

Table 4.4: Thermogravimetric (TGA) data of the unplastized MC-NH₄NO₃ system

Samples	No. of degradation stage	Temperature range (°C)	DTGA _{max} (°C)	% weight loss	
Pure MC	1	25-125		4	Water loss
	2	125-425	321	86	MC decomposed
90MC5AN	1	25-111		7	Water loss
	2	114-205	182	9	AN decomposed
	3	200-425	313	73	MC decomposed
85MC10AN	1	25-100		7	Water loss
	2	100-200	182	11	AN decomposed
	3	200-450	314	72	MC decomposed
80MC15AN	1	25-100		5	Water loss
	2	100-200	180	15	AN decomposed
	3	200-400	314	69	MC decomposed
75MC20AN	1	25-100		7	Water loss
	2	100-209	178	15	AN decomposed
	3	209-450	315	69	MC decomposed
75MC25AN	1	25-100		8	Water loss
	2	100-200	177	32	AN decomposed
	3	200-450	323	51	MC decomposed
70MC30AN	1	25-123		6	Water loss
	2	123-209	174	30	AN decomposed
	3	209-500	322	56	MC decomposed

DTGA: differential thermogravimetric analysis

Figure 4.14 (b) to (g) shows the thermal stability curves for MC doped with 5 to 30 wt.% NH₄NO₃. For polymer-salt complexes, degradation occurs in three stages. As in the thermogram for pure MC sample, the first weight loss is free water loss. The second weight loss for all doped samples in the temperature range 100 – 210 °C is attributed to the decomposition of NH₄NO₃. According to Gunawan and Zhang (2009), the decomposition temperature for NH₄NO₃ is 170 °C with the evolution of NH₃. The third weight loss

between 200 – 450 °C corresponds to the decomposition of MC since from Figure 4.14 (a) MC decomposition occurs between 200 and 450 °C.

4.5 Electrochemical impedance spectroscopy (EIS) analysis

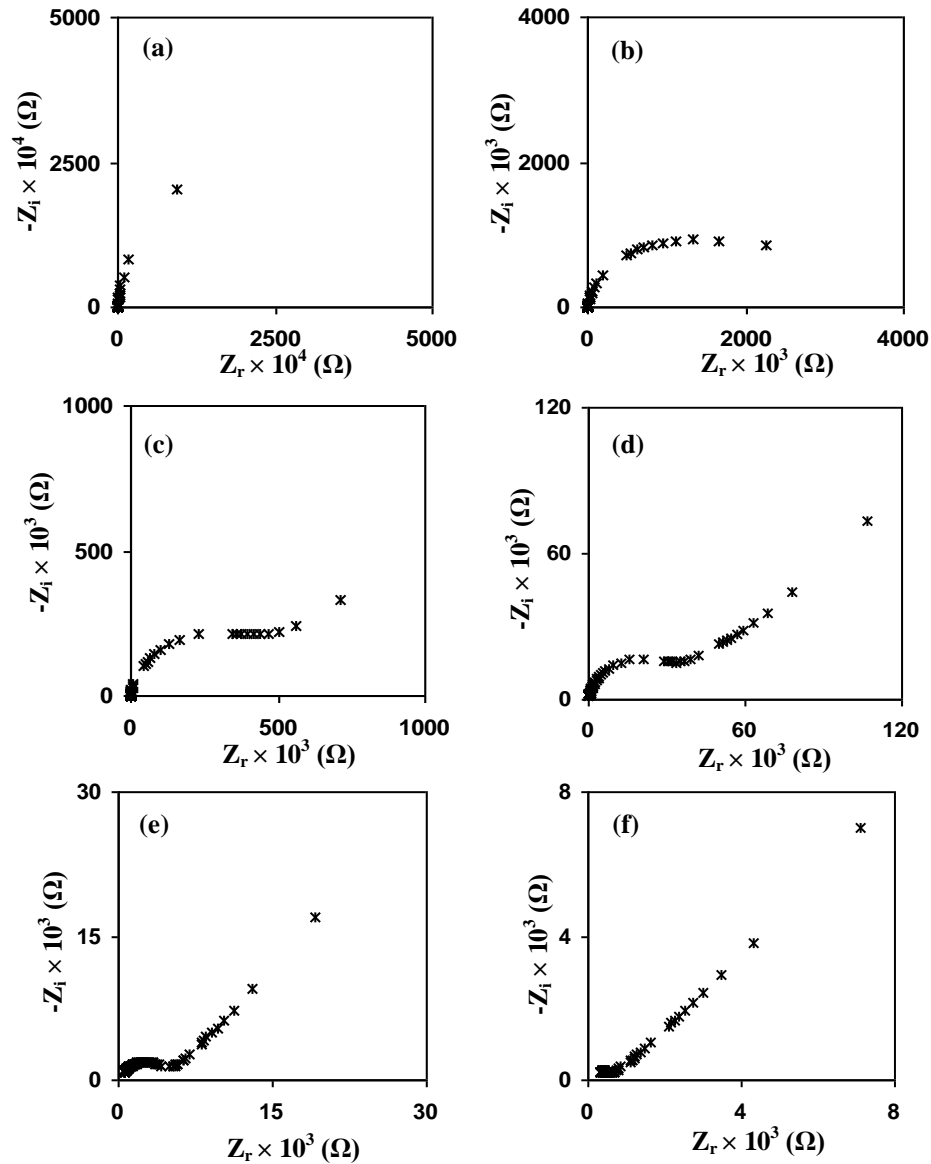
Electrochemical impedance spectroscopy (EIS) is a powerful tool to study the impedance, dielectric, and transport properties of materials [Huang *et al.*, 2010; Macdonald, 2006]. In this section, the HIOKI 3531-01 LCR Hi-Tester interfaced to a computer was used to determine the impedance or bulk resistance in the temperature range 298 K to 373 K. From the equation; $\sigma = t/R_b A$, with σ , t , R_b and A is conductivity, thickness of samples, bulk resistance and area of electrode-electrolyte contact respectively [Kadir *et al.*, 2010; Buraidah *et al.*, 2009], conductivity, σ was calculated. The effect of NH₄NO₃ salt on conductivity was observed. The dielectric properties were studied to understand the conductivity behavior of polymer electrolytes [Ramesh *et al.*, 2002] while transport properties were studied to confirm the conductivity results. Values of mobility and diffusion coefficients can be calculated knowing the number density of mobile ions. Number density of mobile ions can be calculated from the Rice and Roth equation [Rice and Roth, 1972].

4.5.1 The effect of NH₄NO₃ on conductivity of unplasticized MC-NH₄NO₃ system

The impedance plot shows two regions; the semicircle in the high frequency region which is related to the ionic conduction process in the bulk of polymer electrolytes [Hema

et al., 2008] and the spike in the low frequency region suggesting that only capacitive component prevails in the polymer electrolyte.

Figure 4.15 shows the impedance plots for the different concentrations of NH₄NO₃ in MC based polymer electrolyte system at room temperature.



...FIGURE 4.15 CONTINUED...

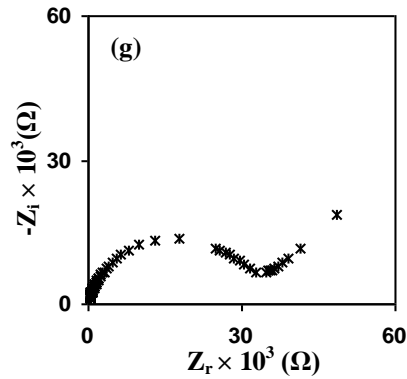


Figure 4.15: Impedance plot of MC-NH₄NO₃ system at room temperature (a) pure MC, (b) 95MC5AN, (c) 90MC10AN, (d) 85MC15AN, (e) 80MC20AN, (f) 75MC25AN, (g) 70MC30AN

The bulk resistance, R_b was evaluated from the intercept of the plot with the real axis. R_b decreases with increase in temperature and with increase in concentration of NH₄NO₃ salt up to a certain optimizing condition. The increase in conductivity with temperature may be attributed to the increase in proton mobility [Viera *et al.*, 2007; Selvasekarapandian *et al.*, 2005]. The variation of room temperature conductivity as the function of NH₄NO₃ concentration in weight percent is depicted in Figure 4.16.

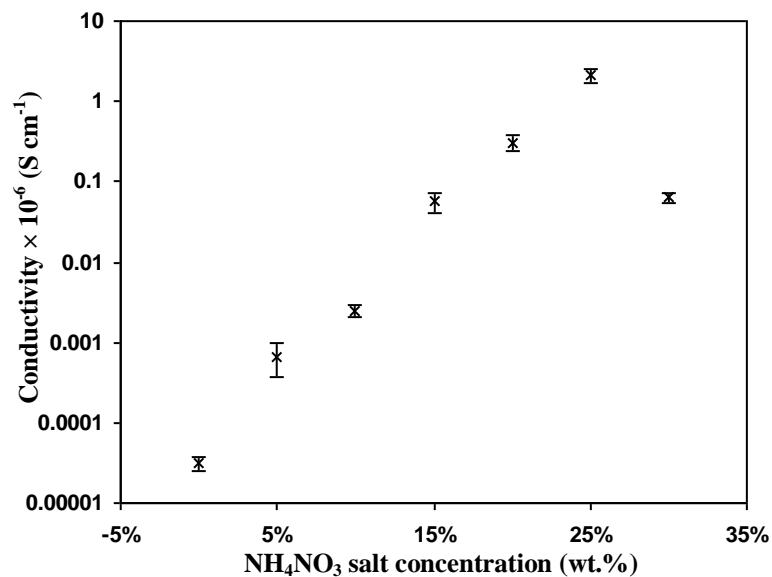


Figure 4.16: Room temperature ionic conductivity of MC doped with NH₄NO₃ salt

Table 4.5 lists the bulk resistance and ionic conductivity value of MC-NH₄NO₃ system at room temperature. The bulk resistance and room temperature conductivity of pure MC is $4.31 \times 10^7 \Omega$ and $3.08 \times 10^{-11} \text{ S cm}^{-1}$ respectively. The bulk resistance decreased by about five orders of magnitude to $7.81 \times 10^2 \Omega$ and conductivity also increased by about five orders of magnitude to $2.10 \times 10^{-6} \text{ S cm}^{-1}$ at 25 wt.% salt concentration.

Table 4.5: The values of bulk resistance, R_b and conductivity, σ of samples with respective composition

(100-x) wt. % MC + x wt. % NH ₄ NO ₃	Designation	Bulk resistance, R_b (Ω)	Conductivity, σ (S cm^{-1})
100 wt. % MC	Pure MC	4.31×10^7	3.08×10^{-11}
95 wt. % MC + 5 wt. % NH ₄ NO ₃	95MC5AN	2.52×10^6	6.74×10^{-10}
90 wt. % MC + 10 wt. % NH ₄ NO ₃	90MC10AN	5.41×10^5	2.49×10^{-9}
85 wt. % MC + 15 wt. % NH ₄ NO ₃	85MC15AN	3.74×10^4	5.75×10^{-8}
80 wt. % MC + 20 wt. % NH ₄ NO ₃	80MC20AN	6.43×10^3	3.10×10^{-7}
75 wt. % MC + 25 wt. % NH ₄ NO ₃	75MC25AN	7.81×10^2	2.10×10^{-6}
70 wt. % MC + 30 wt. % NH ₄ NO ₃	70MC30AN	3.35×10^4	6.40×10^{-8}

From the list above, it can be inferred that, sample 70MC30AN exhibited a decrease in conductivity although more salt has been added. This is in agreement with the x-ray diffractogram of Figure 4.1 and FTIR spectra of Figures 4.5, 4.6 and 4.12 which indicated that the salt has recrystallized and this reduces of the number of mobile ions to act as charge carriers.

4.5.2 Dielectric behavior of room temperature conductivity

The aim of investigating dielectric behavior of methyl cellulose (MC) doped with ammonium nitrate (NH₄NO₃) at room temperature is to understand the conductivity behavior of the polymer electrolyte films [Ramesh *et al.*, 2002]. According to El-Anwar *et al.* (2000), by studying the dielectric behavior, some physico-chemical properties of polymer can be explored. Khiar *et al.* (2006) pointed that the dielectric constant can manifests the increase in number density of charge carriers.

Figure 4.17 and 4.18 show the variation of dielectric constant, ϵ_r and dielectric loss, ϵ_i as a function of frequency for MC-NH₄NO₃ complexes at room temperature.

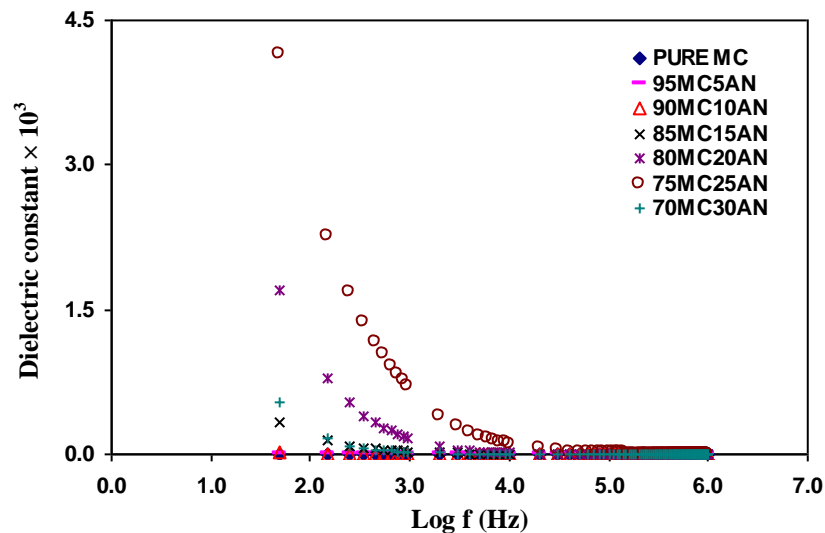


Figure 4.17: Dielectric constant versus log frequency plot for (100-x) MC + x NH₄NO₃ system (x= 5, 10, 15, 20, 25 and 30 wt.%).

It can be seen that for every sample the value of ϵ_r and ϵ_i decreases with increasing frequency. The increase in ϵ_r and ϵ_i at low frequencies is attributed to space charge accumulation due to the long period of the electric field [Ramesh and Ng, 2009; Karan *et al.*, 2008]. In the two figures, no appreciable relaxation peaks are observed in the studied

frequency range. This shows that the increase in conductivity is due to an increase in the number density of mobile ions. The variation in ϵ_r and ϵ_i at low frequencies are observed to follow the same trend as in the conductivity-composition relationship. The sample with the highest conductivity has the highest dielectric constant and dielectric loss.

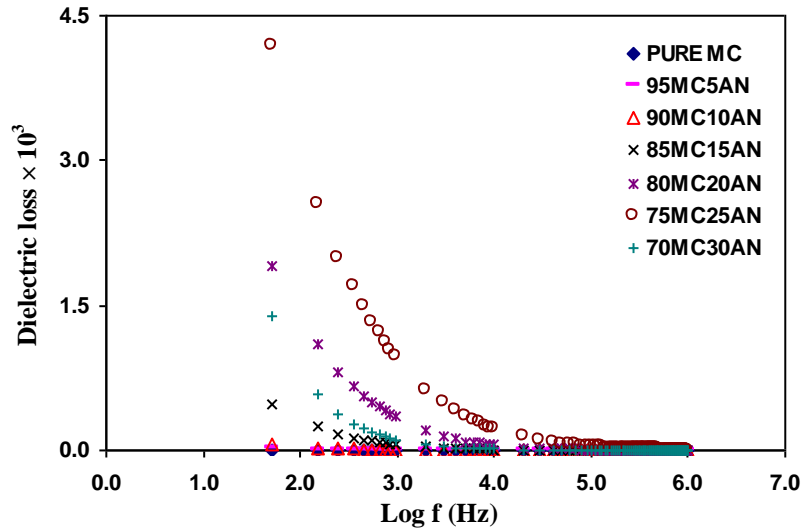


Figure 4.18: Dielectric loss versus log frequency plot for (100- x) MC + x NH₄NO₃ system ($x= 5, 10, 15, 20, 25$ and 30 wt.%)

Depicted in Figure 4.19 is the variation of real part of the electrical modulus (M_r) at room temperature for the various concentration of NH₄NO₃ salt.

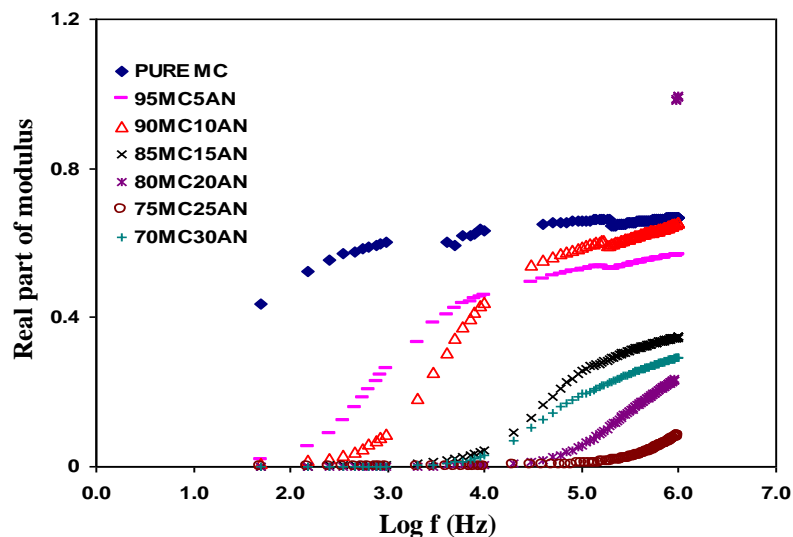


Figure 4.19: Real part of modulus, M_r versus log frequency plot for (100- x) MC + x NH₄NO₃ system ($x= 5, 10, 15, 20, 25$ and 30 wt.%).

Depicted in Figure 4.20 is the variation of imaginary part of the electrical modulus (M_i) at room temperature for the various concentrations of NH₄NO₃ salt. The existence of a long tail towards low frequencies for some samples is attributed to the large capacitance associated with the electrodes [Osman *et al.*, 2001; Gogulamurali *et al.*, 1992]. In M_i versus log frequency plots, the appearance of peaks which correspond to the conductivity relaxation [Pradhan *et al.*, 2009] are observed to shift from low to higher frequency region and it follows the trend in the conductivity variation [Yahya and Arof, 2004]. The presence of such peaks in M_i plots indicates that the electrolyte system is an ionic conductor [Ramesh and Ng, 2009].

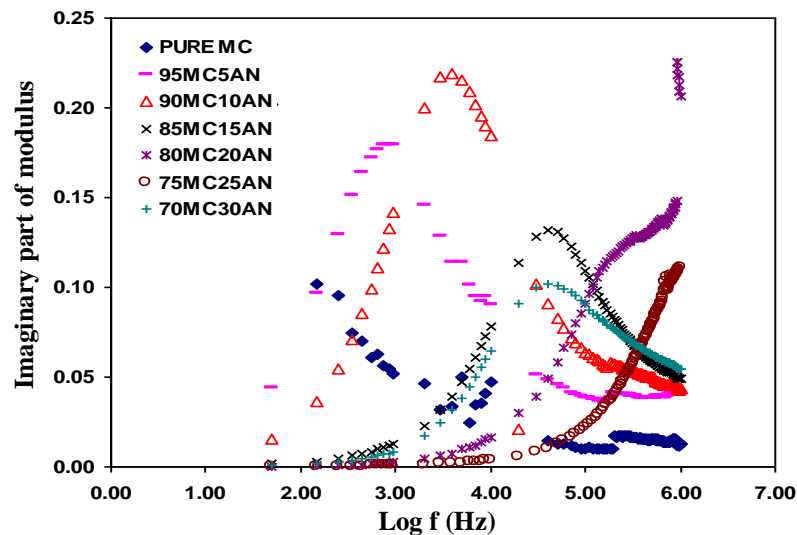


Figure 4.20: Imaginary part of modulus, M_i versus log frequency plot for (100- x) MC + x NH₄NO₃ system ($x = 5, 10, 15, 20, 25$ and 30 wt.%).

A capacitance value can be calculated at the peak frequency of the M_i plots from the relation:

$$M_i = \frac{\epsilon_o}{2C} \quad (4.2)$$

The capacitance values are listed in Table 4.6.

Table 4.6: The values of capacitance, C

Salt concentration (wt.%)	Capacitance (pF)
5	0.25
10	0.20
15	0.33
30	0.43

Figure 4.21 depicts the frequency dependence of loss tangent at room temperature.

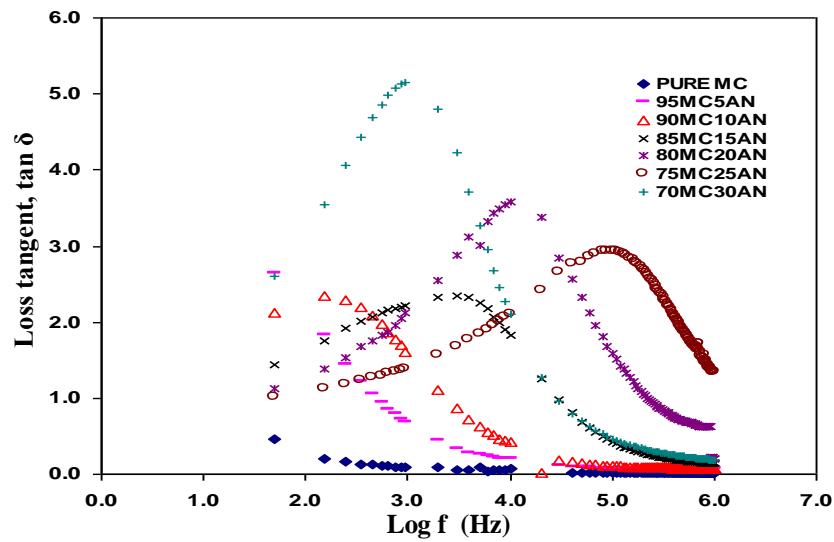


Figure 4.21: Loss tangent versus log frequency plot for (100-x) MC + x NH₄NO₃ system (x= 5, 10, 15, 20, 25 and 30 wt.%)

The angular frequency of the applied field, ω at which the $(\tan \delta)_{\max}$ occurs can be related to the relaxation time for the ionic charge carriers, τ as shown below:

$$\tau \omega = 1 \quad (4.3)$$

Here ω is the angular velocity, $\omega = 2\pi f$, f is the frequency value corresponding to maximum $\tan \delta$. The occurrence of relaxation time is the result of the efforts carried out by ionic charge carriers within the polymer material to obey the change in the direction of applied

field. The shift of $(\tan \delta)_{\max}$ towards higher frequency with increasing conductivity indicates that relaxation time decreases with conductivity as shown in Figure 4.22.

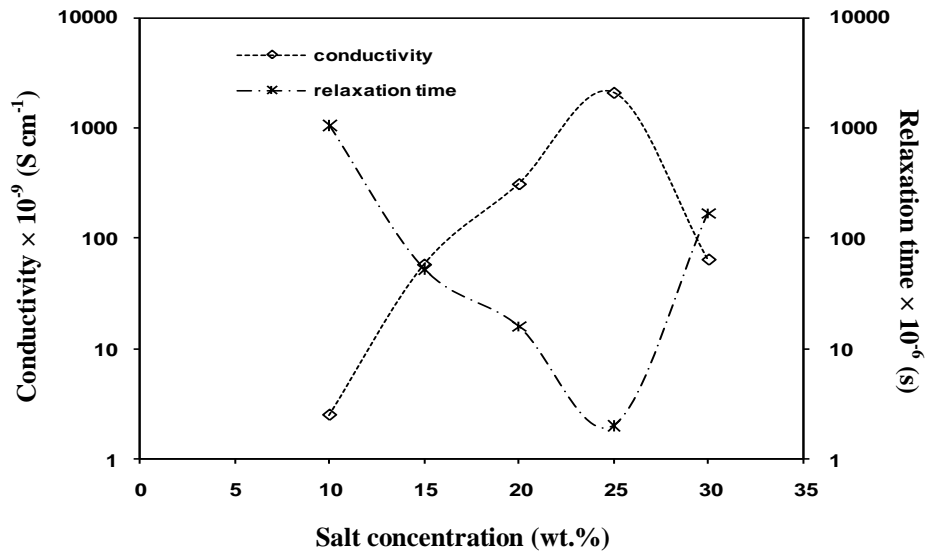
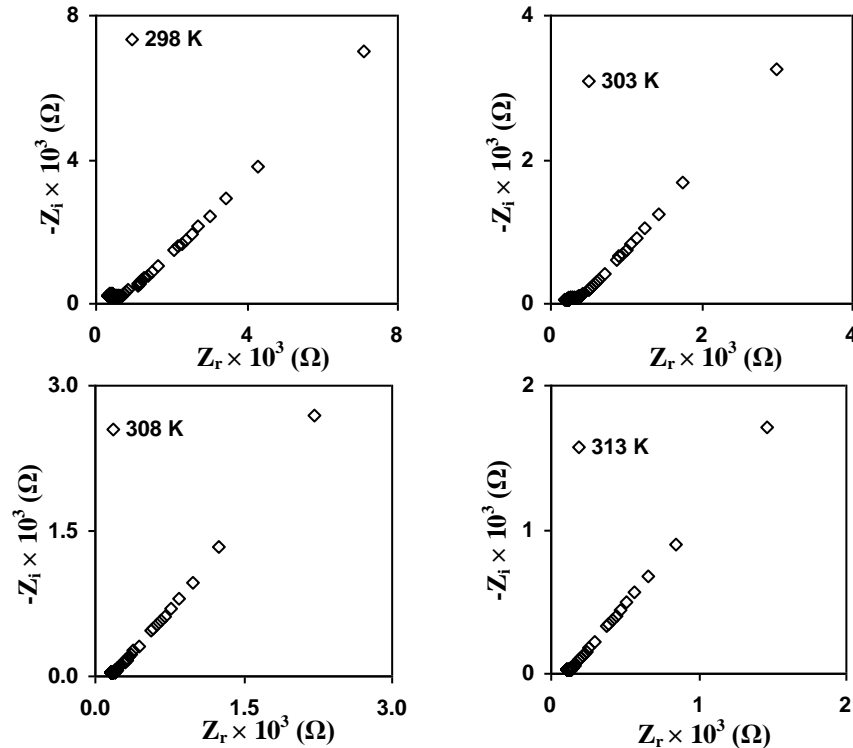
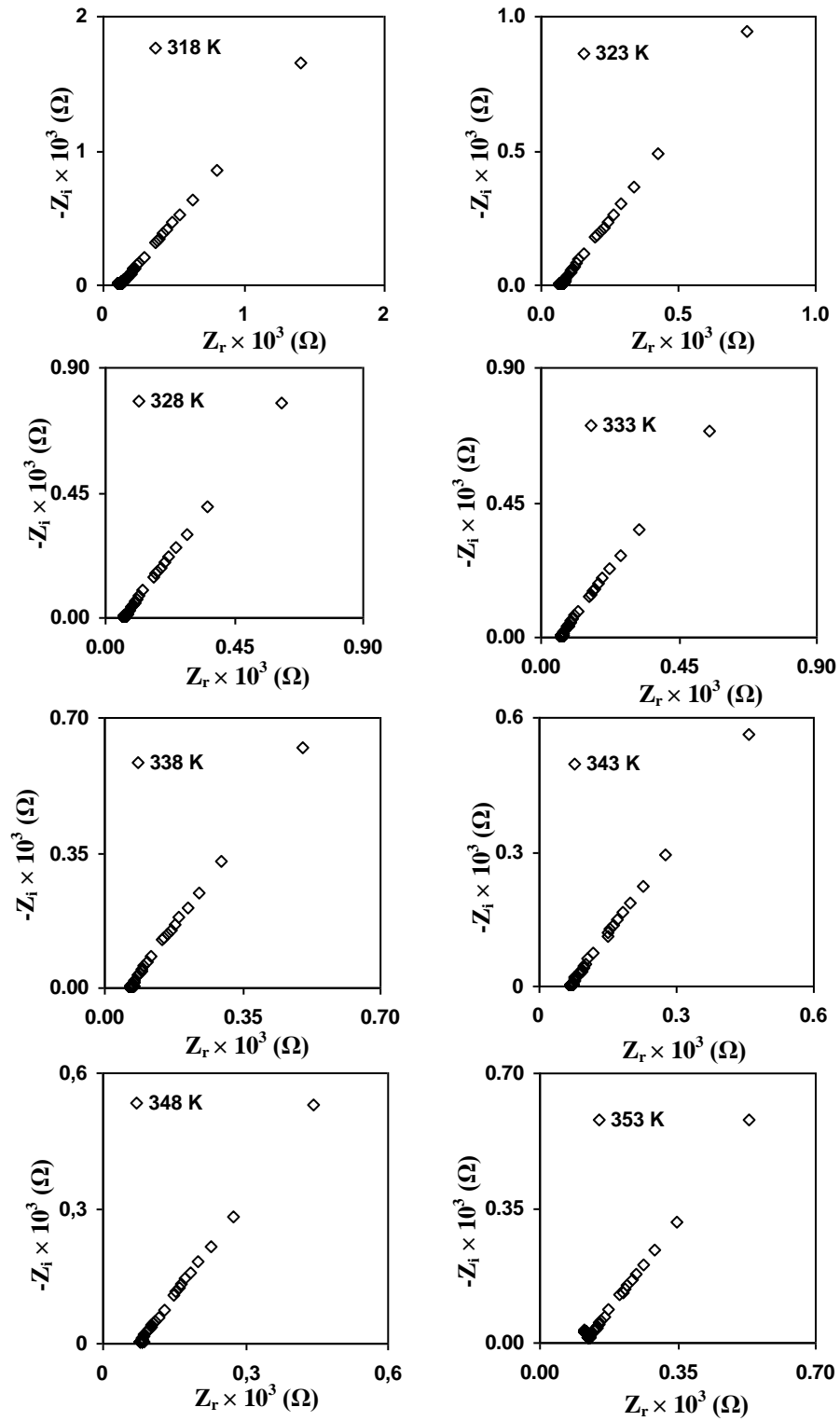


Figure 4.22: The dependence of conductivity and relaxation time on NH₄NO₃ salt concentration at room temperature

4.5.3 The effect of temperature on conductivity of unplasticized MC-NH₄NO₃ system



...FIGURE 4.23 CONTINUED...



...FIGURE 4.23 CONTINUED...

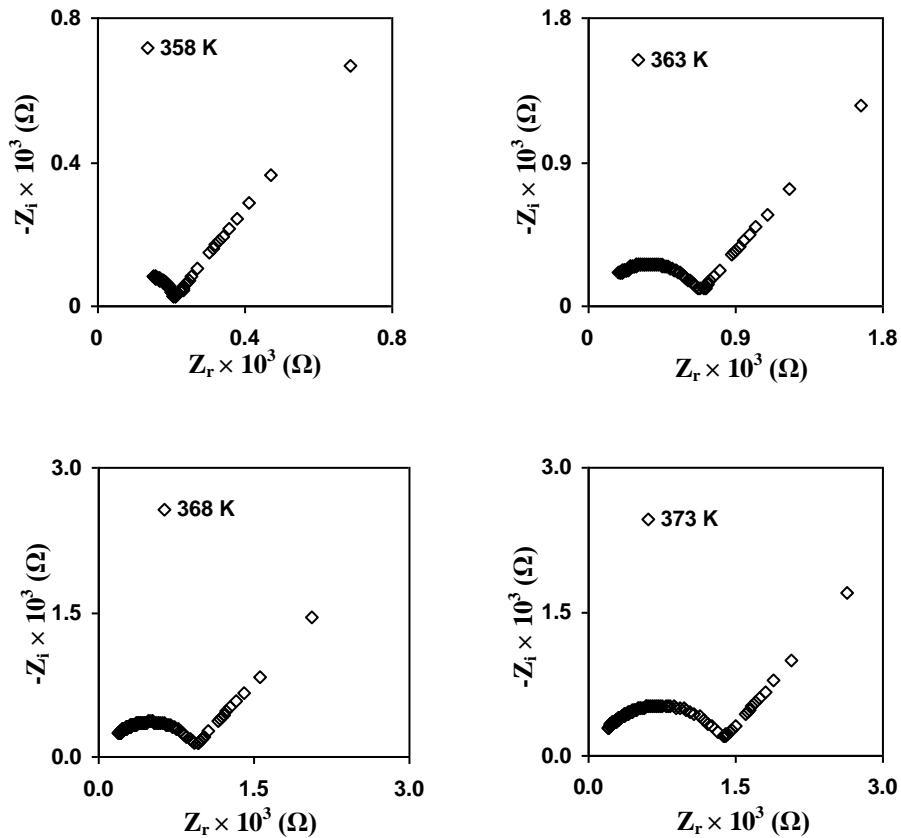


Figure 4.23: Impedance plot of 75 wt.% MC-25wt.% NH₄NO₃ system at various temperature

Figure 4.23 shows impedance plots of the highest conducting polymer electrolyte for MC-NH₄NO₃ system at various temperatures.

Figure 4.24 depicts the variation of conductivity as a function of temperature for MC-NH₄NO₃ polymer electrolyte system. In order to determine whether the conductivity values lie on a straight line or curve, the regression value, r^2 was found using trendline of linear and polynomial lines from Microsoft Excel. r^2 for polynomial is almost 1. After knowing this, the curved lines were manually drawn. It is clear that the temperature dependence of conductivity did not follow Arrhenius rule. The conductivity-temperature relationship is not linear. The conductivity of MC-NH₄NO₃ polymer electrolytes system

can be expressed according to Vogel-Tamman-Fulcher (VTF) rule based on the non-linear relationship between conductivity and temperature as displayed in Figure 4.24.

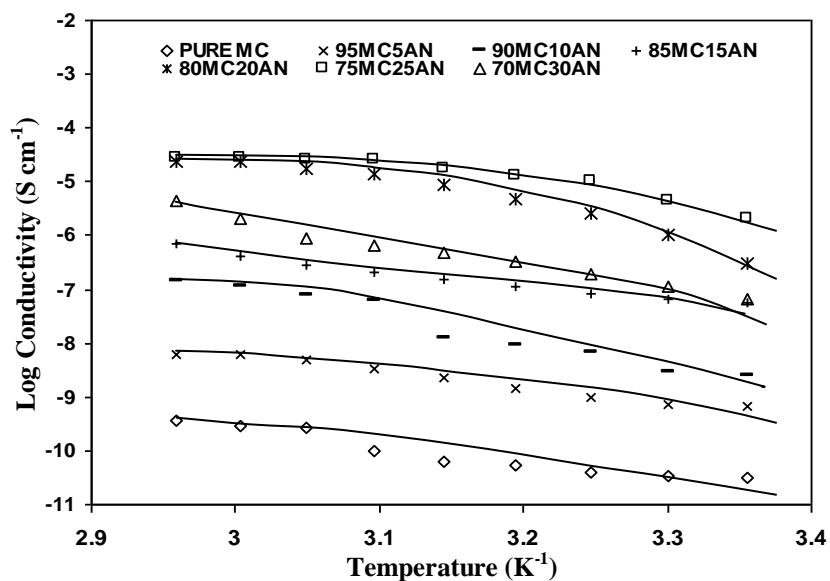


Figure 4.24: Temperature dependence of ionic conductivity for samples of MC doped with various concentrations of NH₄NO₃

Figure 4.25 displays the $\text{Log } \sigma T^{1/2}$ versus $10^3/|T-T_0|$ graphs for all samples except for samples of MC doped with 20 and 25wt. % NH₄NO₃. We were not able to get a good linear fit to the component.

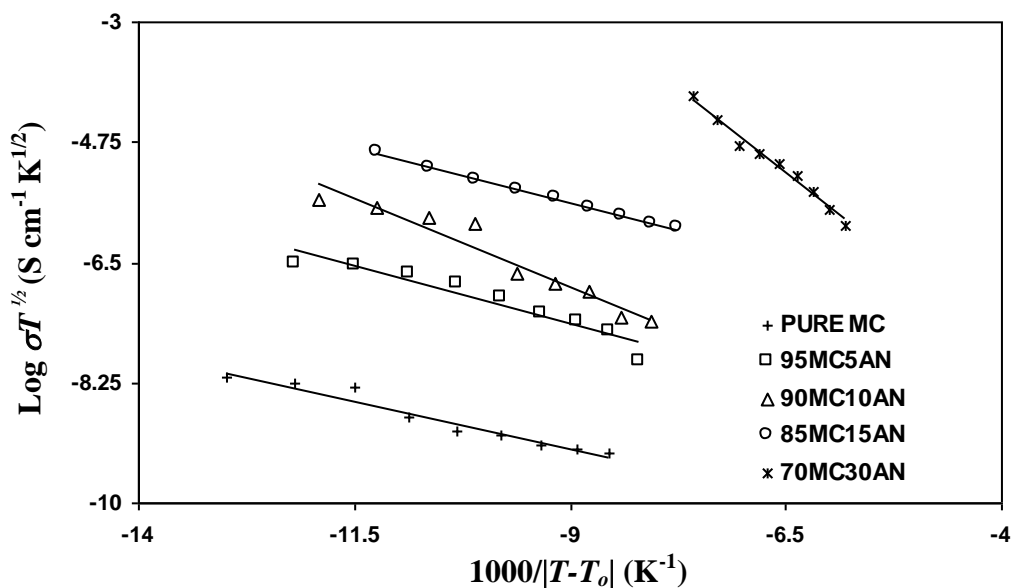


Figure 4.25: Temperature dependence of ionic conductivity for samples of MC doped with various concentrations of NH₄NO₃

4.5.4 The effect of temperature on dielectric behavior

The effect of temperature on dielectric behavior was studied from room temperature, 298 K until 338 K. The variation of the dielectric constant, ϵ_r and dielectric loss, ϵ_i for the highest conducting sample of MC-NH₄NO₃ system, 75MC25AN as a function of frequency at various temperature are depicted in Figures 4.26 and 4.27 respectively.

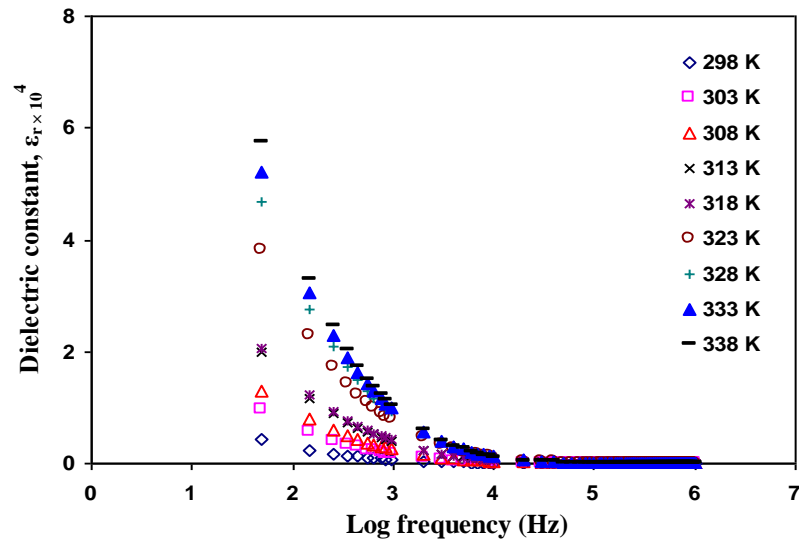


Figure 4.26: Dielectric constant versus log frequency plot for the highest conducting sample in MC-NH₄NO₃ system, 75MC25AN at various temperatures

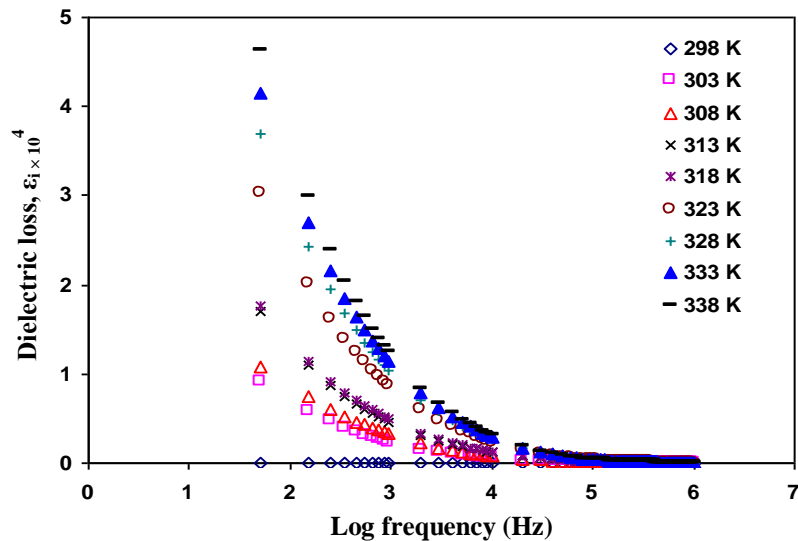


Figure 4.27: Dielectric loss versus log frequency plot for the highest conducting sample in MC-NH₄NO₃ system, 75MC25AN at various temperatures

Dielectric constant represents stored energy and dielectric loss represents the loss of energy due to ion collision. From the figures, as temperature increases dielectric constant and dielectric loss increased.

The real and imaginary parts of modulus as a function of frequency at different temperatures for the highest conducting sample 75MC25AN are shown in Figures 4.28 and 4.29 respectively.

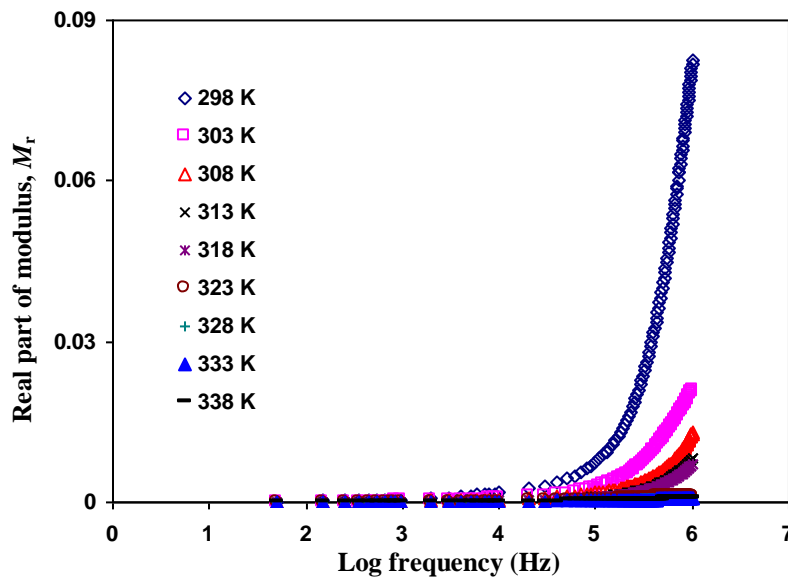


Figure 4.28: Real part of modulus, M_r versus log frequency plot for the highest conducting sample in MC-NH₄NO₃ system, 75MC25AN at various temperatures

From Figure 4.28, M_r increases with increasing frequency. At low frequencies, the value of M_r approaches to zero and according to Ramesh *et al.* (2008), this indicates that the polarization phenomena makes a negligible contribution to M_r . The behavior at low frequency region is attributed to the electrode/electrolyte interfacial and grain boundary effects while the high frequency peak pattern is attributed to the bulk relaxation occurring in the materials [Gogulamurali *et al.*, 1996]. Since no relaxation peak is observed, the loss tangent, $\tan \delta$ formalism will be adopted.

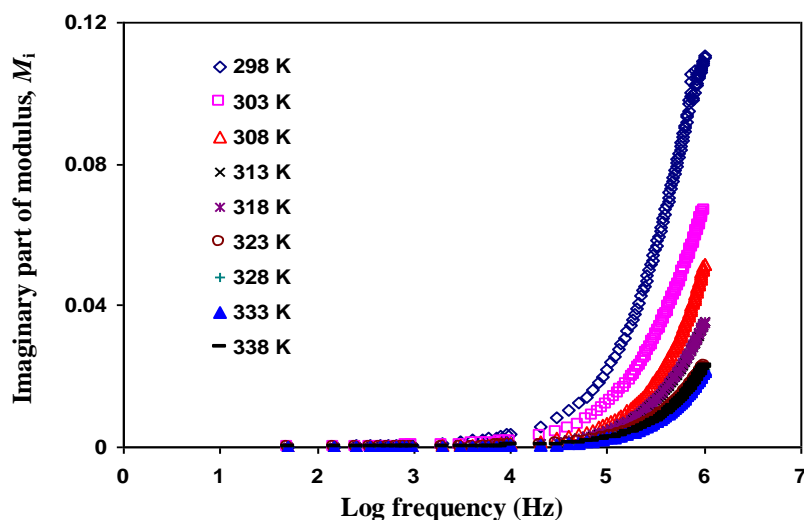


Figure 4.29: Imaginary part of modulus, M_i versus log frequency plot for the highest conducting sample in MC-NH₄NO₃ system, 75MC25AN at various temperatures

Figure 4.30 depicts the plot of $\tan \delta$ as a function of frequency at different temperatures.

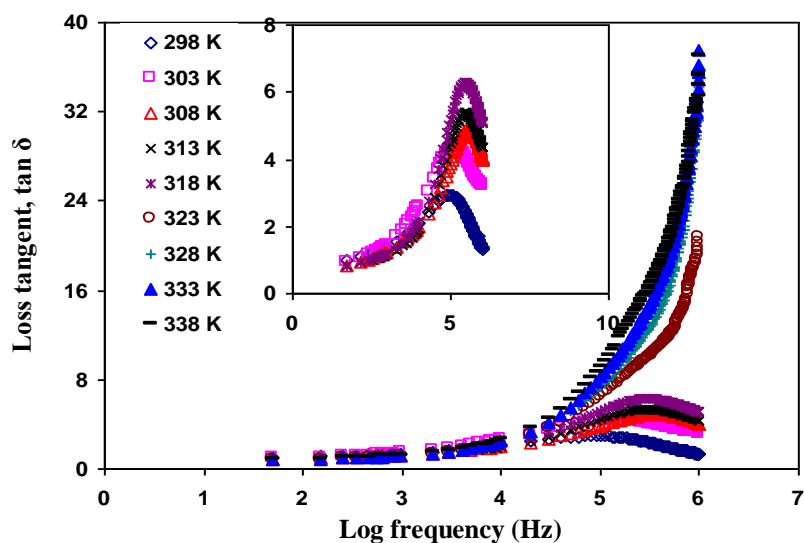


Figure 4.30: Loss tangent versus log frequency plot for the highest conducting sample in MC-NH₄NO₃ system, 75MC25AN at various temperatures

It can be seen that as temperature increases, the maximum of $\tan \delta$, $(\tan \delta)_{\max}$ shifts towards higher frequency and at the same time, the height of maximum increases as

temperature increases. According to Prabakar *et al.* (2003) the increase of height of $(\tan \delta)_{\max}$ with the increasing temperature maybe attributed to the decrease of resistivity of the samples prepared.

The relaxation time, τ for the ionic carrier was determined from the relation:

$$\tau = \frac{1}{\omega} \quad (4.4)$$

The angular frequency of the applied field, ω for various temperatures where $\tan \delta$ is a maximum was obtained from the frequency value. The relaxation time obtained was then plotted as a function of temperature as shown in Figure 4.31.

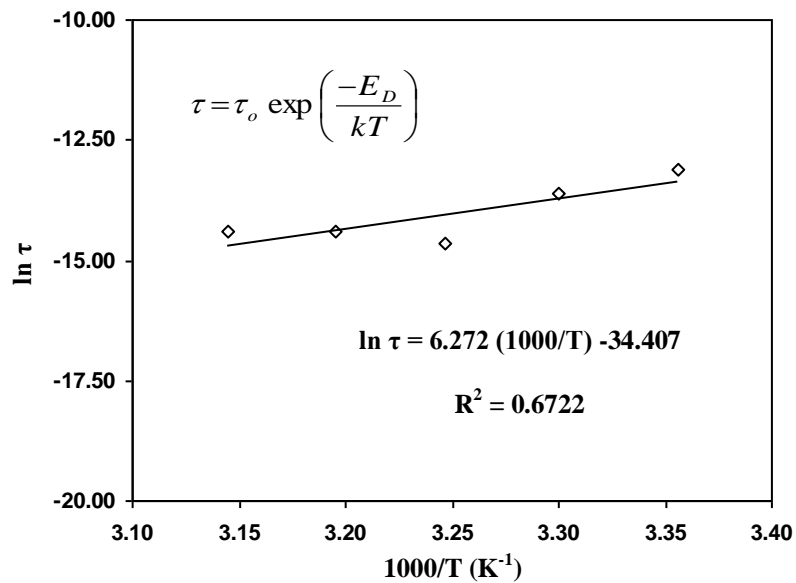


Figure 4.31: Variation of $\ln \tau$ with temperature for the highest conducting sample 75MC25AN in MC-NH₄NO₃ system.

The activation energy for relaxation, E_D was calculated to be 0.54 eV.

Depicted in Figure 4.32 is the normalized plot of $\tan \delta / (\tan \delta)_{\max}$ versus f/f_{\max} at various temperatures for the highest conducting sample, 75MC25AN in MC-NH₄NO₃ system. $\tan \delta$ represents the value of loss tangent at any frequency and $(\tan \delta)_{\max}$ represents

the value of loss tangent at the corresponding f_{\max} . The curves are seen to overlap almost perfectly on a single master curve indicating that all dynamic processes occurring at different temperatures show the same thermal activation energy [Selvasekarapandian and Vijayakumar, 2002]. This normalized plot is very important to know whether activation energy for this sample is the same or not for different temperatures

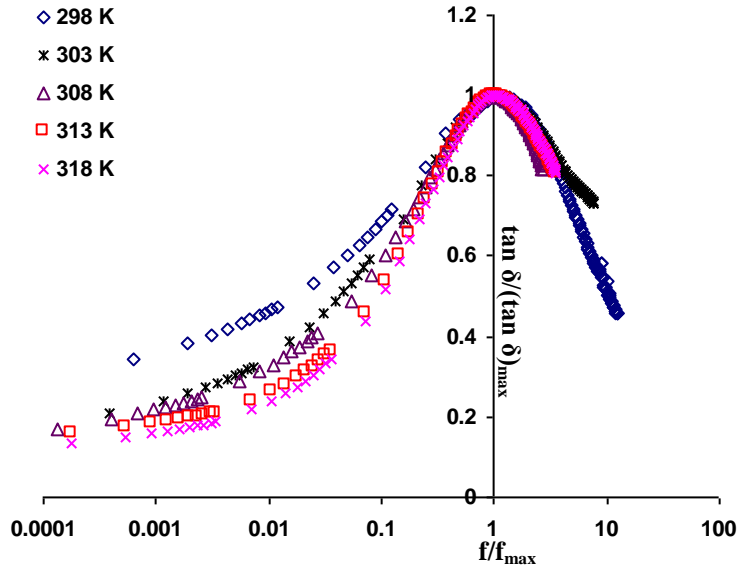


Figure 4.32: Normalized plot of $\tan \delta / (\tan \delta)_{\max}$ versus f/f_{\max} for the highest conducting sample 75MC25AN in MC-NH₄NO₃ system at various temperature.

4.5.5 Effect of glass transition temperature on conductivity and salt concentration

The glass transition temperature can be studied using thermal methods such as differential scanning calorimetry. In this work, we calculate the T_g using the relationship between conductivity and temperature given by the Vogel–Tamman–Fulcher (VTF) rule as

$$\text{Log } \sigma T^{1/2} = \text{Log } A - \frac{E_a}{k_b (T - T_\theta)} \quad (4.5)$$

where σ is conductivity, A is the pre-exponential factor, which is proportional to the number of ionic carriers, E_a is the pseudoactivation energy, T is absolute temperature and k_b is Boltzmann constant. T_o is a quasi-equilibrium glass transition temperature at which free volume disappears. T_o was obtained by trial and error to make the conductivity-temperature data from Figure 4.24 fit the above equation.

In this work T_o is taken to be 50 K lower than the glass transition temperature, T_g . From Rimdusit *et al.* (2008), T_g of MC has been reported to be 449 K. Hence $T_o = 399$ K. To determine T_g for MC-NH₄NO₃ samples, $T_o = 399$ K was substituted into the above equation. Since the points are expected to lie on a straight line, it was necessary to obtain the maximum regression value indicating the points obey above equation. T_o value was changed by trial and error until the maximum regression value was obtained. The regression value for fitting the data points to the straight line obeying the above equation is 0.95 for the pure MC sample, 0.91 for the sample doped with 5 wt.% AN, 0.94 for the sample doped with 10 wt.% AN, ~1 for the sample doped with 15 wt.% AN and 0.99 for the sample doped with 30 wt.% AN. The value of T_o for all samples is shown in Table 4.7.

Table 4.7: T_o value for MC-NH₄NO₃ system

Sample	T_o (K)
Pure MC	415
95MC5AN	420
90MC10AN	422
85MC15AN	427
80MC20AN	439
75MC25AN	453
70MC30AN	470

The conductivity increases as temperature increases in the temperature range from 298 to 333 K as shown in Figure 4.24 from which it can be inferred that conductivity is thermally assisted. From such a line, T_g for the samples doped with 20 and 25 wt.% AN was estimated to be 489 and 503 K, respectively. T_g of pure MC in the present work is 465 K. Rimdusit *et al.* (2008) obtained T_g for pure MC as 449 K using differential scanning calorimetry (DSC) and as 463 K using dynamic mechanical analysis (DMA). Park and Ruckenstein (2001) reported T_g of MC as 472.5 K. The result obtained in the present work using conductivity–temperature data that obeys the VTF equation is in good agreement with the reported results. Depicted in Fig. 4.33 is the graph of glass transition temperature, T_g ($=T_o+50$) against concentration of NH₄NO₃ in weight percentage. T_g increases with increasing concentration of salt.

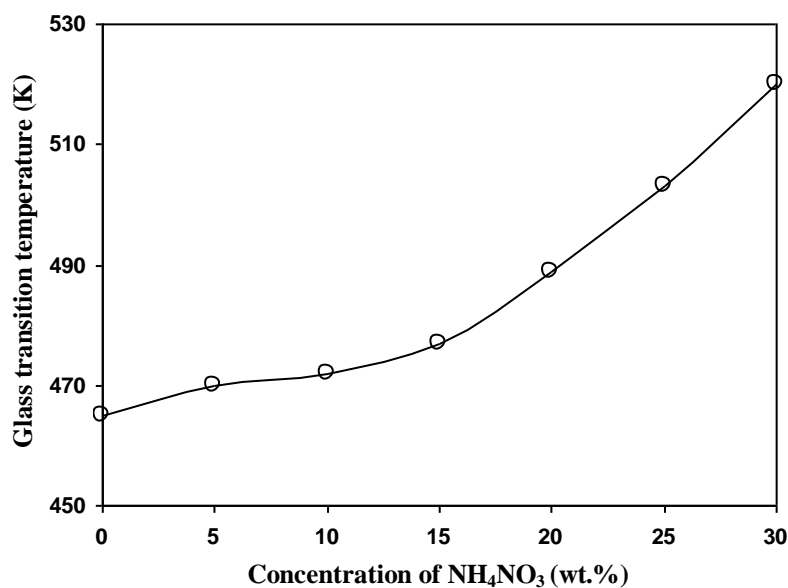


Figure 4.33: The glass transition temperature of MC doped with NH₄NO₃ salt concentration.

4.5.6 Transport parameters of MC-NH₄NO₃ system

Transport parameters were calculated using the conductivity and the Rice and Roth equation [Rice and Roth, 1972]. The basic ionic parameters in transport properties are conductivity, number density and mobility of mobile ions which can be expressed via the equation below:

$$\sigma = nq\mu \quad (4.6)$$

Here σ is ionic conductivity, n is number density of mobile ions, μ is mobility of mobile ions and q is electron charge. Number density of mobile ions is a very important parameter in understanding the transport properties of PEs. The Rice and Roth equation is very suitable to calculate the number density of mobile ions if all other parameters in that equation is already known. The Rice and Roth equation states that conductivity is given by

$$\sigma = \frac{(Ze)^2}{3kT} n v \ell \exp\left(-\frac{E_A}{kT}\right) \quad (4.7)$$

Here $Z = 1$ for proton charge carriers, E_A is the activation energy which can be obtained from the conductivity–temperature relationship in Figure 4.24. k is Boltzmann constant and T is experimental temperature. ℓ is the mean free path or distance between coordinating sites (electron donating atoms) and v is velocity of the free ions. ℓ for MC is 1.5 nm, which was deduced from Yokota *et al.* (2007).

Table 4.8 lists velocity of the ionic charge carrier, τ , and n .

Table 4.8: Transport parameters for MC-NH₄NO₃ system at room temperature

NH ₄ NO ₃ (wt.%)	$\nu = \sqrt{2E_A / m}$ (cm s ⁻¹)	τ (s)	n (cm ⁻³)
5	3.58×10^3	4.19×10^{-11}	8.21×10^{12}
10	4.43×10^3	3.40×10^{-11}	9.67×10^{13}
15	3.47×10^3	4.32×10^{-11}	6.17×10^{14}
20	5.39×10^3	2.78×10^{-11}	6.80×10^{16}
25	4.69×10^3	3.20×10^{-11}	1.26×10^{17}
30	6.14×10^3	2.44×10^{-11}	7.17×10^{16}

m = mass of one hydrogen ion

The lowest conducting sample has the number density of mobile ions of $8.21 \times 10^{12} \text{ cm}^{-3}$ and the highest conducting sample has the number density of mobile ions of $1.26 \times 10^{17} \text{ cm}^{-3}$. It can be seen that the number density of mobile ions increased with addition of NH₄NO₃ and hence increases the conductivity value up to 25 wt.%. Beyond that, number density decreased and conductivity also decreased. Recrystallization of salt out from the polymer contributes to decreasing the number density of mobile ions which can be seen in XRD pattern in Figure 4.1 and FTIR spectra in Figures 4.5 and 4.12. From data in Table 4.8, it can be inferred that conductivity is governed by number density of mobile ions.

Knowing the number density of the mobile ions, the cation mobility can be estimated if the proton transference number is known. Maurya *et al.* (1992) reported that, the transference number, t_{H^+} for protons in the PEO-NH₄ClO₄ electrolyte system ranges from 0.74 to 1.00. Based on the results of Maurya *et al.* (1992) the transference number as a function of weight percentage of ammonium salt was estimated. Figure 4.34 shows the transport number versus concentration of ammonium salt in weight percentage which was replotted from data reported by Maurya *et al.* (1992).

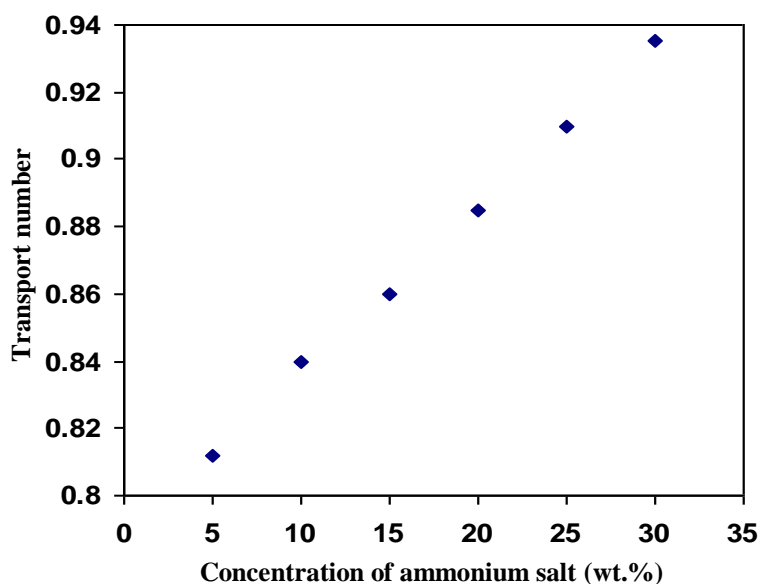


Figure 4.34: The assumed transference number used in this work was based on Maurya *et al.* (1992)

From the definition of t_{H^+} ($\sigma^+ = \sigma t_{H^+}$), mobility of cations, μ^+ can be calculated from

$$\mu^+ = \frac{\sigma^+}{nq} \quad (4.8)$$

where σ^+ is the cation conductivity and n is the number density of mobile ions obtained from the Rice and Roth equation. Results for transport parameters are listed in Table 4.9.

Table 4.9: Transport parameters for MC-NH₄NO₃ system at room temperature

NH ₄ NO ₃ (wt.%)	t_{H^+} (based on Maurya <i>et al.</i> 1992)	n^+ (cm ⁻³)	σ^+ (S cm ⁻¹)	μ^+ (cm ² V ⁻¹ s ⁻¹)
5	0.81	6.64×10^{12}	5.46×10^{-10}	5.13×10^{-4}
10	0.84	8.12×10^{13}	2.09×10^{-9}	1.61×10^{-4}
15	0.86	5.31×10^{14}	4.95×10^{-8}	5.82×10^{-4}
20	0.88	5.98×10^{16}	2.73×10^{-7}	2.85×10^{-5}
25	0.91	1.15×10^{17}	1.91×10^{-6}	1.04×10^{-4}
30	0.94	6.74×10^{16}	6.02×10^{-8}	5.58×10^{-6}

To know whether the number density of mobile charge carriers helps in the conductivity increment when temperature increases, the temperature dependent data was also analyzed using the Rice and Roth equation. Figure 4.35 depicts the number density as a function of temperature. It can be observed that the conductivity is dependent on the number density of mobile ions up to 323 K. Beyond that, the number density decreased. Mobility however increased over the whole temperature range studied (298 K to 373 K). In this system, conductivity only increased until 333 K. It can be concluded that, the number density of mobile ions has greater influence on the conductivity at temperature above 323 K.

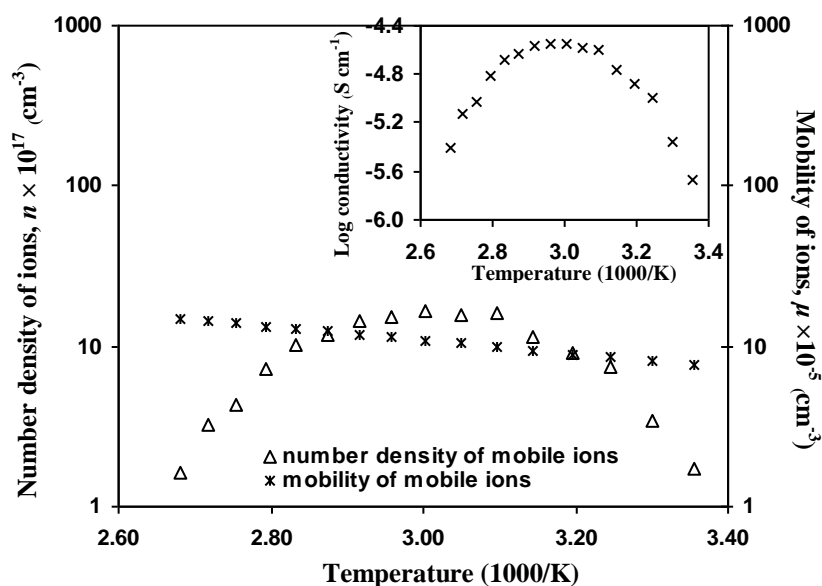


Figure 4.35: Number density of mobile ions, n for the highest conducting sample, 75MC25AN in MC-NH₄NO₃ system as a function of temperature

Figure 4.36 depicts variation of diffusion coefficient of mobile ions against temperature. Due to the small value of diffusion coefficient, it can be inferred that diffusion may not be the mechanism of ionic conduction.

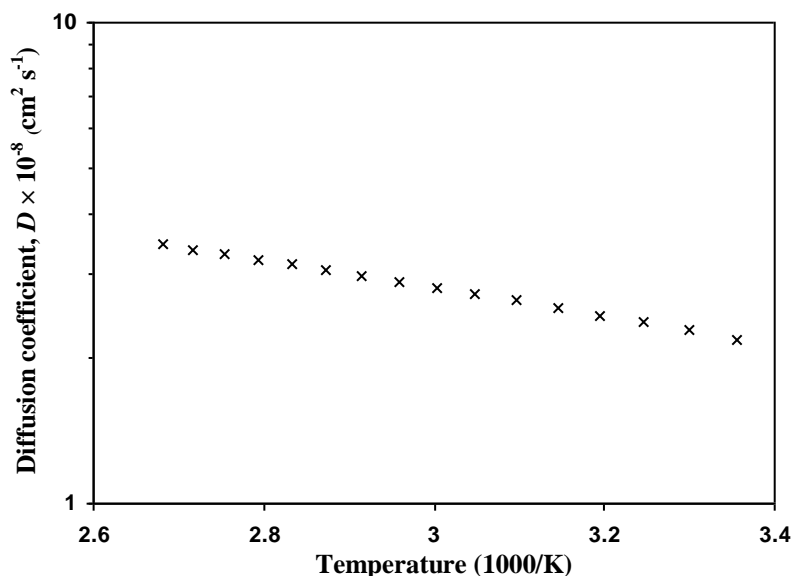


Figure 4.36: Diffusion coefficient of mobile ions, D for the highest conducting sample, 75MC25AN in MC-NH₄NO₃ system as a function of temperature

4.6 Summary

The unplasticized MC-NH₄NO₃ polymer electrolytes system has been prepared by the solution casting technique. The natures of the prepared samples were found to be amorphous at room temperature. The interaction between MC and NH₄NO₃ were detected when a new peak at $2\theta = 8^\circ$ appeared for 5 to 30 wt.% salt. The recrystallization of salt occurred at sample containing 30 wt.% salt and this is inferred when peaks due to NH₄NO₃ appear in the x-ray diffractogram of the sample. FTIR results revealed that the complexation between MC and NH₄NO₃ occurred at oxygen atom in C-O groups when the peak at 1053 cm⁻¹ for pure MC shifted to 1051 cm⁻¹ for 75 wt.% MC-25 wt.% NH₄NO₃. The presence of a small peak at 1040 cm⁻¹ for 70 wt.% MC-30 wt.% NH₄NO₃ sample also shows some interaction between MC and NH₄NO₃. The recrystallization of salt out of the prepared samples can be detected when FTIR spectra of 70 wt.% MC-30 wt.% NH₄NO₃ showed a peak due to pure NH₄NO₃ salt at 827 cm⁻¹. The conductivity for 75MC25AN is higher five magnitude order than pure MC sample with conductivity value is 2.10×10^{-6} S

cm⁻¹. From conductivity-temperature relationship studies, temperature dependence of conductivity is non-Arrhenius behavior. The dielectric properties at room and elevated temperatures were found to be consistent with the trend of conductivity for these samples. The higher conductivity sample gives the highest dielectric constant. The peak in the imaginary part of modulus versus log frequency shows that the samples are ionic conductors. The salt concentration affects the glass transition temperature, T_g . With addition of salt, T_g will increase due to interaction between oxygen atoms of the C-O group in MC and cation of the salt. Transport parameters have been calculated using Rice and Roth model. The number density of mobile ions could be seen as a controller for the conductivity increment at room and elevated temperatures.